

---

# Communication-Efficient Byzantine-Resilient Federated Zero-Order Optimization

---

**Afonso de Sá Delgado Neto**  
Technical University of Munich  
Munich, Germany  
afonso.delgado@tum.de

**Maximilian Egger**  
Technical University of Munich  
Munich, Germany  
maximilian.egger@tum.de

**Mayank Bakshi**  
Arizona State University  
Tucson, AZ, United States  
bakshi@asu.edu

**Rawad Bitar**  
Technical University of Munich  
Munich, Germany  
rawad.bitar@tum.de

## Abstract

We introduce CYBER-0, the first zero-order optimization algorithm for memory- and communication efficient Federated Learning, resilient to Byzantine faults. We show through extensive numerical experiments on the MNIST dataset and fine-tuning RoBERTa-Large that CYBER-0 outperforms state-of-the-art algorithms in terms of communication and memory efficiency while reaching similar accuracy. We provide theoretical guarantees on its convergence for convex loss functions.

## 1 Introduction

Federated Learning [1] is a distributed machine learning approach where a shared model is trained across multiple devices or servers, each holding their own local data, and a central server, called the federator. Rather than transferring the data itself, the devices (called clients) collaboratively update and improve a central model by exchanging model parameters.

Federated Learning (FL) faces several key challenges, such as heterogeneity across clients' data [2], [3], maintaining the privacy of the clients' data [4]–[11], security against Byzantine clients [12]–[16] and communication efficiency [17]–[23]. We focus on jointly maintaining security and communication efficiency, two challenges that have been studied separately in the literature.

Security against Byzantine clients, *i.e.*, clients deliberately corrupting their computation to disrupt the process, is paramount. It is shown in [13] that, if undetected, only one Byzantine client inserting errors is enough to prevent the learning algorithm from converging.

In FL settings, clients run backpropagation on their local data and communicate a  $d$ -dimensional vector (usually  $d$  is in the order of  $10^6$ – $10^9$ ) to the federator, making communication and computation two crucial bottlenecks, especially in settings where the clients are edge devices with limited computation and communication capabilities and energy constraints.

We introduce CYBER-0, a novel communication-efficient and Byzantine-resilient algorithm within the context of zero-order optimization. Zero-order optimization, *i.e.*, optimization techniques that require no gradient computation, has seen significant traction in recent years, *e.g.*, [24]–[28]. Zero-order optimization alleviates both computation and communication costs by allowing clients to send approximations of their gradients using random linear projections as (i) it does not require backpropagation; and (ii) it allows significant compression of the communicated vector.

While [28] achieves communication efficiency through reduced frequencies of model exchanges, we achieve significant communication cost savings by a novel bi-directional shared seed concept, inspired by [24]. As a result, clients and the federator only send  $k$  *real numbers*, for a parameter  $k > 0$ , instead of high-dimensional vectors. This is coupled with an effective robust aggregation technique specifically tailored to the zero-order optimization context.

We validate the effectiveness of CYBER-0 through extensive experiments. For MNIST, we observe the same accuracy as in [15] with a hundred-fold saving in communication. In fine-tuning Large Language Models (LLMs) [26], CYBER-0 achieves high accuracy in the presence of Byzantine clients, together with a million-fold saving in terms of communication compared to uncompressed transmission. The superiority of CYBER-0 in fine-tuning LLMs is motivated by the findings of [24] and [26] in which it is shown that certain problem domains exhibit an inherently low *intrinsic* dimensionality, making zero-order optimization (hence also CYBER-0) a suitable optimization technique. The fast convergence of CYBER-0 aligns with those findings. Furthermore, it was infeasible to compare to state-of-the-art robust FL schemes that require backpropagation as the simulations overloaded the memory of our GPUs of type Nvidia GeForce RTX 4090; highlighting the memory efficiency of CYBER-0. In addition, we theoretically prove that CYBER-0 converges under the assumption of strong convexity.

To our knowledge, this is the first work that simultaneously addresses security and communication/memory efficiency in FL through zero-order methods; offering a unique advantage, particularly in environments where first-order gradient information is not available or not computationally feasible due to memory-constrained client devices.

## 2 Problem Setting

We start with notation and conventions used in the paper.

**Notation.** Vectors are represented by boldface letters, *e.g.*,  $\mathbf{z}$  and sets are denoted by calligraphic letters, *e.g.*,  $\mathcal{W}$ . The  $L_2$  norm of a vector  $\mathbf{w}$  is denoted by  $\|\mathbf{w}\|_2$ . The inner product of vectors  $\mathbf{z}$  and  $\mathbf{w}$  is represented interchangeably by  $\langle \mathbf{z}, \mathbf{w} \rangle$  and  $\mathbf{z}^\top \mathbf{w}$ , chosen to enhance the clarity of exposition. The  $i$ -th coordinate of a vector  $\mathbf{w}$  is denoted by  $w^{(i)}$ . The natural logarithm is represented by  $\log$ .

We define  $[n] \triangleq \{1, \dots, n\}$  and  $\mathbb{S}^d$  as the set of unit-norm vectors in  $\mathbb{R}^d$ , *i.e.*,  $\mathbb{S}^d = \{\mathbf{x} \in \mathbb{R}^d : \|\mathbf{x}\|_2 = 1\}$ . Given a convex set  $\mathcal{W} \subseteq \mathbb{R}^d$ , the Euclidean projection of a vector  $\mathbf{w} \in \mathbb{R}^d$  on  $\mathcal{W}$  is  $\Pi_{\mathcal{W}}(\mathbf{w}) \triangleq \operatorname{argmin}_{\mathbf{w}' \in \mathcal{W}} \|\mathbf{w}' - \mathbf{w}\|_2^2$ . We denote the operation of uniformly sampling a vector  $\mathbf{z}$  from  $\mathbb{S}^d$  as  $\mathbf{z} \sim \mathbb{S}^d$ . Similarly, sampling independently and uniformly a set of vectors  $Z = \{\mathbf{z}_1, \mathbf{z}_2, \dots, \mathbf{z}_n\}$  is denoted as either  $Z \sim \mathbb{S}^d$  or  $\mathbf{z}_1, \mathbf{z}_2, \dots, \mathbf{z}_n \sim \mathbb{S}^d$ .

**Federated Learning.** The model consists of a network comprising of a federator and  $m$  clients, denoted by the indices  $\{1, 2, \dots, m\}$ . Each client  $i$  has a set of data samples  $\mathcal{D}_i \triangleq \{\gamma^{i,1}, \dots, \gamma^{i,|\mathcal{D}_i|}\} \subseteq \Gamma$ , where  $\Gamma$  is the data space. Let  $\mathcal{D} \triangleq \bigcup_{i \in [m]} \mathcal{D}_i$  be the global dataset. The loss function, denoted by  $f(\mathbf{w}; \gamma)$ , is defined with respect to the parameter vector  $\mathbf{w} \in \mathcal{W} \subseteq \mathbb{R}^d$  and a data vector  $\gamma \in \Gamma$ .

The federator exchanges messages with clients over multiple rounds with the goal of minimizing the statistical loss  $\hat{F}(\mathbf{w}) = \frac{1}{|\mathcal{D}|} \sum_{\gamma \in \mathcal{D}} f(\mathbf{w}, \gamma)$ . At training step  $t \geq 0$ , the federator sends a model vector  $\mathbf{w}^t$  to the clients. Each client  $i$  then computes an update message  $\mathbf{g}_i^t$  based on the federator's model vector  $\mathbf{w}^t$  and its local dataset  $\mathcal{D}_i$  and sends the result back to the federator. Finally, the federator updates the model to  $\mathbf{w}^{t+1}$  as a function of  $\mathbf{w}^t$  and  $\{\mathbf{g}_i^t : i \in [m]\}$ . At the end of training step  $T$ , the federator outputs its learned model  $\mathbf{w}^T$ .

**Adversarial Model.** Byzantine clients behave as in Definition 2.1. A fraction  $\alpha m$  (unknown to the federator),  $0 \leq \alpha < 1/2$ , of the clients are Byzantine. Byzantine clients' indices are denoted by  $\mathcal{B}$ .

**Definition 2.1** (Attack Model). A Byzantine client  $b \in \mathcal{B}$  has complete knowledge of the vectors transmitted by all other clients to the federator at each training step. Given this knowledge, it may send arbitrary vectors to the federator, denoted as  $*$ , aiming to disrupt the optimization procedure.

---

**Algorithm 1** CYBER-0

---

**Input:**  $w_0 \in \mathcal{W}$  is the initial model parameter vector,  $\beta$  is the trimmed mean factor,  $\eta$  is the learning rate,  $\mu$  is the perturbation step,  $k$  is the number of samples per estimate and  $T$  is the total number of learning steps.

**for**  $t = 0$  **to**  $T$  **do**

**► Federator**

        Samples  $Z^t = \{z_1^t, z_2^t, \dots, z_k^t\} \sim \mathbb{S}^d$

        Distributes  $w^t = w^t$  to each client

**for**  $i = 0$  **to**  $m$  **in parallel do**

        ▷ **client**  $i$

**for each**  $z_r^t \in Z^t$  **do**

                Compute and send  $g_i(w^t, z_r^t)$  to federator, cf. Definition 3.1

**end for**

**end for**

**► Federator**

$\hat{g}^t \leftarrow \frac{1}{k} \sum_{r=1}^k \hat{g}_\beta(w^t, z_r^t) z_r^t$

$w^{t+1} \leftarrow \Pi_{\mathcal{W}}(w^t - \eta_t \hat{g}^t)$

**end for**

---

### 3 Robust Zero-Order Federated Learning

We introduce CYBER-0, a Byzantine-resilient federated zero-order optimization. CYBER-0 builds on the principles of MeZO [26], a memory-efficient centralized algorithm. In addition to providing Byzantine resilience, CYBER-0 significantly improves the communication efficiency compared to FedZO [28], the FL counterpart of MeZO. CYBER-0 is given in Algorithm 1 and is explained next.

While the components of CYBER-0 are separately well-studied, their successful combination yields subtle but significant complexities. Extending centralized zero-order algorithms to Byzantine-resilient FL requires ensuring that the choice of the vectors  $z_1, \dots, z_k$  does not compromise resiliency and still allows convergence. In addition, proving that the robustness of a trimmed mean operation, meant to operate on the coordinates of gradient vectors, extends to the zero-order estimator requires novel theoretical tools. Further challenges include practical validation of the proposed algorithm and investigating zero-order fine-tuning in federated large language models. We provide next a formal explanation of the main concepts and the algorithm.

**Definition 3.1** (Zero-Order estimate). For a given  $\mu \geq 0$ , a vector  $z \in \mathbb{S}^d$  and a loss function  $f(w, \gamma)$ , the *single-sample zero-order estimate* of the gradient  $\nabla f(w, \gamma)$  is defined as

$$g(w, z, \gamma, \mu) = \begin{cases} d \frac{f(w+\mu z; \gamma) - f(w-\mu z; \gamma)}{2\mu} z, & \text{for } \mu > 0, \\ d \langle \nabla f(w, \gamma), z \rangle z, & \text{for } \mu = 0. \end{cases}$$

As we consider a fixed  $\mu$  throughout the paper, we write  $g(w, z, \gamma)$  instead of  $g(w, z, \gamma, \mu)$ .

To simplify notation, for each client  $i \in [m]$  and each  $j \in [D_i]$ , we define the client partial estimate as  $g_{i,j}(w, z) \triangleq g(w, z, \gamma^{i,j})$  and the *client estimate* as  $\mathbf{g}_i(w, z) \triangleq \frac{1}{|D_i|} \sum_{j=1}^{|D_i|} g_{i,j}(w, z)$ .

We define the norms  $g_i(w, z) \triangleq \|g_i(w, z)\|_2$  and  $g(w, z, \gamma, \mu) \triangleq g(w, z, \gamma, \mu)$ .

**Definition 3.2** (Trimmed Mean (adopted from [15])). Given  $0 \leq \beta < 1/2$  and a multiset  $X = \{x_1, x_2, \dots, x_m\}$ , the trimmed mean operation is defined as  $\text{TrMn}_\beta \{X\} \triangleq \frac{1}{m-2\lfloor \beta m \rfloor} \sum_{x \in X_\beta} x$ , where  $X_\beta$  is obtained by removing the largest and smallest  $\lfloor \beta m \rfloor$  elements from  $X$ .

**Computation Procedure.** At training step  $t$ , the federator shares the model  $w^t$  and  $k$  vectors  $z_1^t, \dots, z_k^t \sim \mathbb{S}^d$  with the clients. Client  $i$  computes  $\mathbf{g}_i(w^t, z_r^t)$  and sends  $g_i(w^t, z_r^t)$ ,  $r \in [k]$ , to the federator. Byzantine clients send arbitrary vectors denoted by  $*$ . The robust aggregation proceeds as follows. For each  $r \in [k]$ , the federator first computes  $\hat{g}_\beta(w^t, z_r^t)$  as

$$\hat{g}_\beta(w^t, z_r^t) \triangleq \text{TrMn}_\beta \{ \{g_i(w^t, z_r^t) : i \in [m] \setminus \mathcal{B}\} \cup \{* : i \in \mathcal{B}\} \}.$$

Next, the federator computes the gradient estimate  $\hat{g}^t = \frac{1}{k} \sum_{r=1}^k \hat{g}_\beta(w^t, z_r^t) z_r^t$  and updates the model as  $w^{t+1} = \Pi_{\mathcal{W}}(w^t - \eta_t \hat{g}^t)$  for a given learning rate  $\eta_t$ . To reduce the communication cost, the federator can only broadcast  $\hat{g}_\beta(w^t, z_r^t)$ ,  $\forall r \in [k]$  and each client reconstruct  $w^{t+1}$  individually.

### 3.1 Properties of CYBER-0

Our proposed algorithm exhibits Byzantine resilience and communication and memory efficiency. Those are notable properties contributing to its effectiveness in federated learning.

**Byzantine Resilience.** A key component of our robust aggregation is that it aligns with the compression mechanism used by the clients. The transmitted values can be perceived as a linear  $k$ -dimensional compressed representation of the gradient. This format is inherently amenable to scalar robustness procedures, such as the trimmed mean.

**Communication Efficiency.** CYBER-0 compresses  $d$ -dimensional vector into  $k$  real values, offering low communication costs. At first glance, CYBER-0 appears to rely on transmitting the  $d$ -dimensional vectors  $z_1^t, \dots, z_k^t$  at each training step. However, this overhead is efficiently mitigated through a simple yet effective strategy: utilizing a shared common seed among clients and the federator. The federator disseminates this seed, which is then used by the clients to sample the perturbation directions  $z_1^t, \dots, z_k^t$  in a coordinated manner. Local updates (such as those in [28]) can further reduce the communication cost. For clarity of exposition, we provide CYBER-0 with local updates in Algorithm 4 in the appendix, together with corresponding numerical experiments.

**Memory Efficiency.** By using Zero-order approximation, which inherently does not necessitate backpropagation, CYBER-0 saves significantly on memory (by up to a factor of 12) compared to traditional training methods relying on backpropagation, cf. [26]. Furthermore, CYBER-0 adopts in-place perturbations on model parameters, a technique also used in MeZO [26], to further reduce memory usage.

Under a different setting,  $\mu = 0$ , CYBER-0’s gradient estimates are computed by projecting the true gradient along different directions. This removes the memory efficiency property in exchange for better computational efficiency, since instead of calculating  $2k$  function evaluations, only a single gradient and  $k$  projection calculations are needed.

To the best of our knowledge, CYBER-0 is the first application of Byzantine resilience in zero-order compressed information scenarios. In contrast, for any case other than  $k = 1$ , coordinate-wise methods [29] do not allow the same compression mechanism to occur in the federator-to-client communication.

Despite its advantages, our algorithm provides a weak privacy guarantee of the clients’ data ensured by the fact the clients only transmit a harshly compressed version of the gradient estimate. Ensuring strong privacy guarantees are known to have a tension with ensuring robustness [30]–[32]. Investigating privacy, robustness and compression is a very interesting future research direction. While fairness can be favored by robust aggregation and enhanced through regularizers to the loss function, pruning outliers may pose additional challenges. Thoroughly analyzing the fairness guarantee is out of the scope of this work.

## 4 Experiments

We present a series of experiments showing the performance of CYBER-0 across various scenarios. First, we employ a Logistic Regression model on MNIST [33] to investigate the parameters’ influence on the convergence of CYBER-0. This setting serves as a foundational test with insights into the baseline performance and parameter sensitivities of CYBER-0 in a controlled environment. For a more comprehensive understanding of CYBER-0’s performance reaching towards advanced applications in Natural Language Processing (NLP), we extend our examination to federated fine-tuning of large language models (LLMs).

While Algorithm 1 completely specifies the behavior of CYBER-0, Appendix A.1 presents an extended algorithm utilized for our experiments, highlighting the memory and communication optimizations in our implementation. The basic functionality of the algorithm remains unchanged.

### 4.1 Experimental Setup

The key conditions for our experiments are client data distribution and simulating Byzantine behaviors, explained next. General simulation parameters and hyperparameters are shown in Appendix

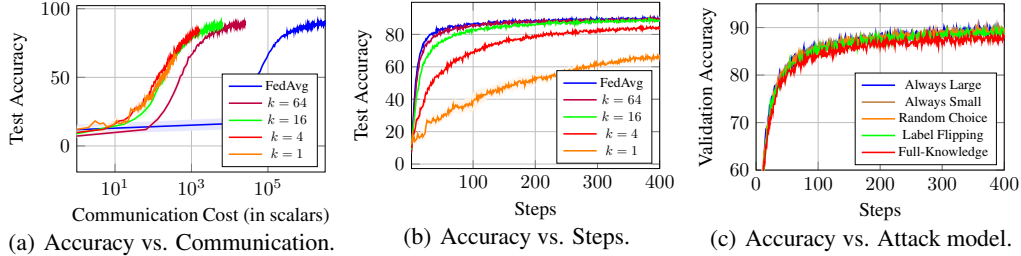


Figure 1: CYBER-0 for logistic regression on MNIST under non-IID data distribution. Figures (a) and (b) show the convergence for varying  $k$  in the absence of Byzantine clients compared to federated averaging (FedAvg). Figure (c) shows different attacks for  $k = 64$  and  $\alpha = \beta = 0.25$ .

A.2. Tables and figures displaying standard deviation measures (denoted by the  $\pm$  sign) represent the average outcomes of three independent simulation runs, initialized by different random seeds.

**Data Distribution.** We investigate two distinct data distribution scenarios: independent and identically distributed (IID) data and non-IID data. In the IID scenario, data labels are uniformly distributed across all participating clients, ensuring an equal representation of each label in the local datasets. Conversely, in the non-IID scenario, we assign a unique label set to each client, thereby creating a skewed label distribution and introducing additional complexity in the learning process.

**Byzantine Behavior.** We consider a worst-case scenario wherein Byzantine clients are fully aware of the communication protocol and the transmissions of other clients. Byzantine clients can collude and act in a deliberately adversarial manner. Our approach draws inspiration from the attack model described in [34], *i.e.*, focusing on maximizing the local gradient deviation at each training step. This is achieved by strategic manipulation of the information sent to the federator. In this attack, the Byzantine clients compute the true gradient estimate obtained from the honest clients. If that estimate is positive, they all send a value equal to the  $\lfloor \beta m \rfloor$ -th smallest honest gradient value. Otherwise, they all send a value equal to the  $\lfloor \beta m \rfloor$ -th largest honest gradient value. This attack is called Full Knowledge and described in Algorithm 3.

For the MNIST experiments, we compare this choice to other Byzantine behaviors to display its effectiveness. In particular, we compare it to three model poisoning strategies: Always Small, Always Large, and Random Choice, in which Byzantine clients all send either the  $\lfloor \beta m \rfloor$ -th smallest, largest or randomly pick one of them, respectively, for each perturbation direction. And a data positioning strategy, Label Flipping, in which the Byzantine devices switch each MNIST label from  $\ell$  to  $9 - \ell$ .

## 4.2 CYBER-0 with Logistic Regression on MNIST

We explore the effect of the sample size  $k$  and the clients’ behavior on the convergence of CYBER-0. We then compare CYBER-0 with coordinate-wise trimmed mean [15], which comes closest in spirit.

**Impact of Sample Size  $k$ .** The training loss trajectories for diverse settings of the sample size parameter  $k$  are illustrated in Figure 1(a) over the cost of communication, and in Figure 1(b) over the number of steps. We include the conventional federated averaging (FedAvg) [1] as a benchmark.

Table 1: Comparison with state-of-the-art: We compare the test accuracies of CYBER-0 ( $k = 64$ ) with the trimmed mean and Krum algorithms. We use  $\beta = \alpha$  for all experiments, the Full-Knowledge attack for CYBER-0, and the model poisoning attacks described in [34] for trimmed mean and Krum.

ALGORITHM	$\alpha = 0.125$	$\alpha = 0.25$	$\alpha = 0.375$
KRUM	69.2 $\pm$ 1.6	10.2 $\pm$ 1.2	6.9 $\pm$ 2.5
TRIMMED MEAN	86.6 $\pm$ 0.3	74.8 $\pm$ 1.1	36.0 $\pm$ 4.1
CYBER-0	87.1 $\pm$ 0.8	80.8 $\pm$ 1.0	60.3 $\pm$ 2.9

Table 2: CYBER-0 in adversarial (CYBER-0, Byzantine) and non-adversarial settings.

	NON-DISTRIBUTED [26]	CYBER-0			
		NON-BYZANTINE		BYZANTINE	
		IID	NON-IID	IID	NON-IID
SST-2	93.3± 0.7	93.1± 0.3	93.1± 0.2	92.9± 0.4	92.7 ±0.4
TREC	94.3± 1.3	95.4± 0.3	95.8± 0.4	92.1± 1.5	78.2± 0.7
SNLI	83.0 ± 1.0	84.8 ± 0.3	84.6 ± 0.7	80.0 ± 0.4	60.1 ± 4.9

We observe a notable trend: as the value of  $k$  increases, the convergence rate progressively aligns with that of standard SGD. This aligns with theoretical expectations in Section 5, as a larger sample size  $k$  yields a sample mean that more closely approximates the true gradient of the loss function.

**Effect of Byzantine Client Behavior.** In Figure 1(c), we present a comparative analysis of the training loss dynamics under different Byzantine client behaviors. Our results show that the Full-Knowledge strategy presents the highest damage to the training process by causing the most substantial delay in convergence. This phenomenon underscores the potency of informed adversarial behaviors in disrupting the learning process.

**Comparison with State-of-the-Art.** We compare the performance of CYBER-0 with the trimmed mean [15] and Krum [13]. For this comparison, we apply the Full-Knowledge attack on CYBER-0, while applying the model poisoning attacks from [34] for the state-of-the-art approaches, as those are the most effective attacks against the respective algorithms. The results are shown in Table 1.

CYBER-0 provides better Byzantine resilience for all  $\alpha$  values while achieving a roughly 100-fold communication reduction. It can be assumed that the projection over the random directions leaves fewer degrees of freedom for the Byzantine clients to change the aggregated gradient, hence providing good Byzantine resilience and allowing for communication efficiency.

### 4.3 Fine-Tuning Language Models with CYBER-0

Following a methodology similar to [26], we utilize the RoBERTa-large model [35] for three distinct NLP tasks: sentiment analysis, natural language inference (NLI) and topic classification. For sentiment analysis, we employ the SST-2 dataset [36]. For NLI, we employ the SNLI dataset [37]. For topic classification, we use the TREC dataset [38]. We adopt a prompt-based fine-tuning approach in a few-shot learning framework, as outlined by [39]. Fine-tuning LLMs is well-established in the literature. The details are omitted here for brevity, interested readers are referred to [39] for details.

We use a set of 512 data points distributed among the clients according to the specified data distribution pattern. These experiments intend to show the applicability of CYBER-0 in more complex and real-world scenarios, particularly in the increasingly relevant field of NLP.

In the classical theory of zero-order optimization [40], fine-tuning LLMs is deemed to be of prohibitively slow convergence due to the role exercised by the model dimension  $d$ . Nevertheless, as evidenced by the findings of [24] and [26], certain problem domains exhibit an inherently low *intrinsic* dimensionality. The fast convergence of CYBER-0, cf. first and second columns of Table 2, aligns with the findings of [24] and [26].

**Robustness of CYBER-0.** The ability of CYBER-0 to mitigate the effect of Byzantine clients, using the strong Full-Knowledge attack, can be seen in the right-most column of Table 2. In IID settings, CYBER-0 exhibits a small drop in accuracy. However, for non-IID settings, while still converging, CYBER-0 exhibits a drop in accuracy in the presence of Byzantine clients. This behavior aligns with the literature on non-IID robust FL. The main reason is that the non-IID data distribution is reflected in the clients’ message updates. Making the distinction between malicious gradients and outliers more challenging. In addition to affecting the final accuracy, Byzantine clients also decrease the convergence speed of the algorithm. We illustrate this effect on the SST-2

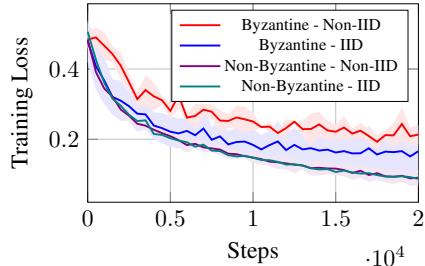


Figure 2: Effect of Byzantine clients on the convergence speed of CYBER-0.

Table 3: Varying the number of samples ( $k$ ) and the number of clients ( $m$ ) in SST-2 using RoBERTa-large in the presence of Byzantine clients with non-IID data distribution.

$k$	TOTAL STEPS	TEST ACCURACY	$m$	BYZANTINE CLIENTS	TEST ACCURACY
1	20,000	$92.7 \pm 0.4$	8	2	$92.7 \pm 0.4$
2	10,000	$92.5 \pm 0.3$	16	4	$92.5 \pm 0.4$
4	5,000	$92.8 \pm 0.5$	32	8	$92.3 \pm 0.6$
8	2,500	$92.7 \pm 0.5$			

experiment in Figure 2, which complements the data presented in Table 2. Similar figures for the SNLI and TREC experiments are given in Appendix A.3.

We further demonstrate communication optimizations and scalability aspects of CYBER-0 using RoBERTa-large on the SST-2 dataset. We vary the number of samples per training step and the total number of clients, cf. Table 3. We provide in Appendix A.4 an extra set of experiments regarding local epochs [1].

**Number of Samples.** As observed in Table 3, and consistent with findings from Section 4.2, for fixed values of  $m = 8$  and  $\beta = 0.25$ , an increase in the number of samples  $k$  correlates with accelerated convergence in terms of steps. CYBER-0 presents here a tradeoff between computational workload and communication efficiency. A larger value of  $k$  necessitates more forward passes per training step. However, the transmission of these passes in batches potentially enhances communication efficiency by reducing the need for frequent synchronization rounds.

**Number of Clients.** We explore the impact of scaling the number of clients while maintaining the same ratio of Byzantine to non-Byzantine clients. As observed in Table 3, for fixed values of  $k = 1$  and  $\beta = 0.25$ , increasing the number of clients does not significantly affect the final test accuracy. This outcome aligns with the expectation that similar data distribution among non-Byzantine clients would result in consistent learning patterns, regardless of the network size.

## 5 Theoretical Analysis

To complement our extensive numerical results, we provide a theoretical convergence guarantee for CYBER-0 for convex loss functions and IID data distribution. The results under those assumptions quantify the interplay between convergence guarantee and the choice of  $\mu$ ,  $k$ , and  $d$  in well-behaved settings and pave the way to an extended analysis for non-convex losses and non-IID data distribution.

Adopting an approach akin to [15], we establish a probabilistic bound on the distance between the robust gradient estimation yielded by our method and the ideal expected gradient obtained in a Byzantine-free context. With such a bound established, we carry a convergence analysis for an SGD algorithm that operates under bounded-error conditions, using the zero-order gradient estimate.

### 5.1 Preliminaries

To establish theoretical results, we make an assumption on the data distribution and define the population loss and the zero-order population estimate.

**Assumption 5.1** (IID Data Distribution). Each client  $i$  has a set of  $n$  data samples  $\{\gamma^{i,1}, \dots, \gamma^{i,n}\}$  sampled from a common data distribution  $D$ .

**Definition 5.2** (Population Loss). The population loss  $F(\mathbf{w})$  is expressed as the expected value of the loss over  $D$ , i.e.,  $F(\mathbf{w}) = \mathbb{E}_{\gamma \sim D}[f(\mathbf{w}; \gamma)]$ .

Associated with the population loss, we have the following optimization problem

$$\mathbf{w}^* = \underset{\mathbf{w} \in \mathcal{W}}{\operatorname{argmin}} F(\mathbf{w}). \quad (1)$$

**Assumption 5.3** (Local Minimum). The model  $\mathbf{w}^*$  is a local minimum of  $F$ .

**Definition 5.4** (Zero-Order Population Estimate). Let  $F$  be the population loss for the optimization problem in (1), then we define the zero-order population estimate by:

$$\bar{\mathbf{g}}(\mathbf{w}, \mathbf{z}) = \mathbb{E}_{\gamma \sim D}[\mathbf{g}(\mathbf{w}, \mathbf{z}, \gamma)] = \begin{cases} d \frac{F(\mathbf{w} + \mu \mathbf{z}) - F(\mathbf{w} - \mu \mathbf{z})}{2\mu} \mathbf{z}, & \text{for } \mu > 0, \\ d \langle \nabla F(\mathbf{w}), \mathbf{z} \rangle \mathbf{z}, & \text{for } \mu = 0, \end{cases}$$

and its norm by  $\bar{g}(\mathbf{w}, \mathbf{z}) = \|\bar{\mathbf{g}}(\mathbf{w}, \mathbf{z})\|_2$ .

## 5.2 Robustness Error Bound

We proceed by deriving the aforementioned bound. We start by adding three assumptions on the functions  $g$ ,  $f$  and  $F$  and the parameter space  $\mathcal{W}$ .

**Assumption 5.5** (Smoothness). Consider any  $\mu \geq 0$ ,  $\gamma \in \Gamma$ ,  $\mathbf{w} \in \mathbb{R}^d$ , and  $\mathbf{z} \in \mathbb{S}^d$ . We assume that  $g(\cdot, \mathbf{z}, \gamma)$  exhibits  $L_{w,\mu}$ -Lipschitz continuity, that  $g(\mathbf{w}, \cdot, \gamma)$  exhibits  $L_{z,\mu}$ -Lipschitz continuity and that  $f(\cdot, \gamma)$  is  $L$ -smooth. Additionally, it is assumed that  $F(\cdot)$  demonstrates  $L_F$ -smoothness. For simplicity of notation, we denote  $\hat{L}_\mu = L_{w,\mu} + L_{z,\mu}$ .

**Assumption 5.6** (Sub-Exponentiality). For all  $\mu \geq 0$ ,  $\mathbf{z} \in \mathbb{S}^d$ , and  $\mathbf{w} \in \mathcal{W}$ ,  $g(\mathbf{w}, \mathbf{z}, \gamma)$  is distributed as a  $v$ -sub-exponential random variable, conditioned upon  $\gamma$  being sampled from  $\mathcal{D}$ .

**Assumption 5.7** (Restriction on  $\mathcal{W}$ ).  $\mathcal{W}$  is both convex and compact with a predefined diameter  $D$ .

With these assumptions in place, we are now positioned to establish a bound on the discrepancy between the robust estimate and the expected estimate among benign clients.

**Theorem 5.8** (Robustness Error Bound). *Let  $\mu \geq 0$ ,  $\mathbf{z} \in \mathbb{S}^d$ ,  $\epsilon > 0$ . Then for any  $\mathbf{z}_r \in \mathbb{S}^d$  for  $r \in [k]$ , under Assumptions 5.5, 5.6,  $\alpha \leq \beta < \frac{1}{2} - \epsilon$ , and with probability at least  $1 - \frac{4}{(1+2nm\hat{L}_\mu)^d(1+nm\hat{L}_\mu D)^d}$*

$$\left\| \frac{1}{k} \sum_{r=1}^k \hat{g}_\beta(\mathbf{w}, \mathbf{z}_r) \mathbf{z}_r - \frac{1}{k} \sum_{r=1}^k \bar{\mathbf{g}}(\mathbf{w}, \mathbf{z}_r) \right\|_2 \leq \Delta,$$

for

$$\Delta \triangleq \sqrt{\log(1+nm\hat{L}_\mu D) + \log(1+2nm\hat{L}_\mu) + \frac{1}{d} \log m} \times \frac{v\sqrt{d}}{\epsilon} \left( \frac{3\beta}{\sqrt{n}} + \frac{\sqrt{2}}{\sqrt{nm}} \right) + \tilde{O} \left( \frac{\beta}{n} + \frac{1}{mn} \right).$$

The proof of Theorem 5.8 is found in Appendix B.1

## 5.3 Convergence analysis

To study the convergence properties of the proposed algorithm, we explore how the algorithm behaves in scenarios with different values of the parameter  $\mu$  under the assumption of strong convexity.

**Assumption 5.9** (Strong-Convexity).  $F(\mathbf{w})$  is  $\lambda$ -strongly convex.

Under this premise, we proceed to analyze the convergence characteristics of Algorithm 1 for  $\mu = 0$ .

**Theorem 5.10** (Convergence,  $\mu = 0$ ). *Assume  $\mu = 0$ ,  $\epsilon > 0$ , set  $\tau = \frac{d+k-1}{\tau L_F}$  and  $\eta = \frac{1}{\tau L_F}$  in Algorithm 1, let  $\mathcal{Z}^t = \{\mathbf{z}_1^t, \mathbf{z}_2^t, \dots, \mathbf{z}_k^t\}$  be the  $k$  uniformly and independently sampled vectors from  $\mathbb{S}^d$  and let  $\mathcal{Z}^t = \bigcup_{i=0}^t \mathcal{Z}^i$ . Under Assumptions 5.5, 5.6, and 5.9, with the constraint  $\alpha \leq \beta < \frac{1}{2} - \epsilon$ , and a probability of at least  $1 - \frac{4}{(1+2nm\hat{L}_\mu)^d(1+nm\hat{L}_\mu D)^d}$ , we have:*

$$\mathbb{E}_{\mathcal{Z}^T} [\|\mathbf{w}^T - \mathbf{w}^*\|_2] \leq \left( 1 - \frac{\lambda}{\tau(L_F + \lambda)} \right)^T \|\mathbf{w}^0 - \mathbf{w}^*\|_2 + \frac{2}{\lambda} \Delta$$

where  $\mathbf{w}^T$  is the parameter vector at the  $T$ -th step and  $\Delta$  is the same as defined in Theorem 5.8.

The proof of this theorem is presented in Appendix B.2.

To achieve an order-optimal error rate of  $\tilde{O}(\frac{\beta}{\sqrt{n}} + \frac{1}{\sqrt{nm}})$ , as suggested by [15], where the  $\beta$  term represents the introduced error by the Byzantine behavior, the number of training steps  $T$  should be at least  $\frac{\tau(L_F + \lambda)}{\lambda} \log(\frac{\lambda}{2\Delta} \|\mathbf{w}^T - \mathbf{w}^*\|_2)$ .

Consistent with zero-order theory [40], [41], our analysis reveals a linear dependence of the convergence rate on the model dimension  $d$ , not observed in first-order methods. This dependence is encapsulated in the parameter  $\tau$ . As the number of sampled perturbation directions  $k$  increases, our algorithm approximates the standard first-order rate of convergence.

Next, we examine the case where  $\mu > 0$ .



**Definition 5.11** (Smoothed Version of  $F$ ). Let  $F$  be a population loss, for any  $\mu > 0$  and  $\mathbf{w} \in \mathbb{R}^d$ . The *smoothed version* of  $F$ ,  $F_\mu : \mathbb{R}^d \rightarrow \mathbb{R}$  is defined as  $F_\mu(\mathbf{w}) = \mathbb{E}_{\mathbf{z} \sim \mathcal{S}^d} [F(\mathbf{w} + \mu\mathbf{z})]$ .

**Assumption 5.12** (Local Minimum of  $F_\mu$ ).  $\mathbf{w}_\mu^* = \arg \min_{\mathbf{w} \in \mathcal{W}} F_\mu(\mathbf{w})$  is local minimum of  $F_\mu$ .

It can be shown (Lemma 4.1(b) of [41]) that for any  $\mathbf{w}$ ,  $F(\mathbf{w})$  and  $F_\mu(\mathbf{w})$  cannot differ more than  $\frac{L\mu^2}{2}$ , implying that the solutions  $F(\mathbf{w}^*)$  and  $F(\mathbf{w}_\mu^*)$  can be made arbitrarily close by the choice of  $\mu$ .

**Theorem 5.13** (Convergence,  $\mu > 0$ ). Assume  $\mu > 0$ , set  $\tau = \frac{2d+(k-1)(1+\sqrt{d})}{k}$  and  $\eta = \frac{1}{2\tau L_F}$  in Algorithm 1 and let  $\mathcal{Z}^t$  be as in Theorem 5.10. Under Assumptions 5.5, 5.6, and 5.9, with  $\alpha \leq \beta < \frac{1}{2} - \epsilon$ , and a probability of at least  $1 - \frac{4}{(1+2nm\bar{L}_\mu)^d(1+nm\bar{L}_\mu D)^d}$ , we have:

$$\mathbb{E}_{\mathcal{Z}^T} [\|\mathbf{w}^T - \mathbf{w}_\mu^*\|_2] \leq \left(1F - \frac{\lambda}{2\tau(L_F + \lambda)}\right)^T \|\mathbf{w}^0 - \mathbf{w}_\mu^*\|_2 \frac{2}{\lambda} \Delta + \frac{8\sqrt{2}\mu d L_F}{\lambda} \sqrt{1 + \frac{\tau}{4}},$$

where  $\mathbf{w}^T$  is the parameter vector at the  $T$ -th step of Algorithm 1 and  $\Delta$  is as defined in Theorem 5.8.

The proof of Theorem 5.13 is found in Appendix B.3.

Similar to the results for  $\mu = 0$ , with  $\mu > 0$ , we observe the same order-optimal error rate under appropriate conditions for  $T$ . Notably, for  $k = 1$ , the convergence rate scales linearly with the dimension  $d$ . However, unlike the case with  $\mu = 0$ , increasing  $k$  does not entirely mitigate this linear dependency, leaving a residual term proportional to  $\sqrt{d}$ .

## 6 Related Work

**Zero-order Optimization.** In recent years, zero-order optimization has significantly evolved, broadening its applicability across various domains. This technique has been particularly instrumental in areas such as black-box optimization [25], [42] and reinforcement learning [24], [43] as gradient computations are not required.

A novel and notable application has emerged with the fine-tuning of LLMs [26], showcasing the versatility of zero-order optimization as a memory-efficient technique to allow the fine-tuning of billion-parameter models, while only using a fraction of the memory required by the first-order counterparts. The federated counterpart was studied in [28].

**Communication Efficiency.** Communication efficiency through gradient compression, can be mainly divided into two categories: quantization-based methods [18], [44], [45], and sparsification-based methods [19], [20]. None of those, however, are tailored for zero-order estimates, in the sense that they act on the  $d$ -dimensional gradients.

Our work relies on compression on the gradient estimate by transmitting only the difference in perturbation losses, while taking advantage of an agreed randomness. We map it back to the work of [24], passing through [26] and [46].

**Byzantine Resilience.** To mitigate adversarial conditions in the learning process, recent research has seen a surge in the development of Byzantine resilient algorithms [13], [15], [47], [48]. Our work is closely related to [15], which applies one-dimensional coordinate-wise statistical robustness techniques to the gradient information transmitted by the clients. In contrast, our countermeasure is applied for each perturbation, posing new theoretical challenges and bridging zero-order estimation and statistical robustness.

**Poisoning attacks.** From the wide range of attacks applied to Byzantine-resilient algorithms, we specially mention data poisoning [49], [50] and model manipulation [34]. Both attacks enable Byzantine clients to effectively reduce the speed of convergence, increase the error rate, or completely disrupt the optimization result. Our attack model is related to [34], in which the Byzantine clients use the full information about the other clients' responses to maximize the deviation from the benign estimate in each optimization step.

## 7 Conclusion

In this paper, we have introduced CYBER-0, a novel federated zero-order optimization scheme designed to withstand Byzantine behaviors. We demonstrated its effectiveness even under challenging conditions, which include a coordinated full-knowledge attack on non-IID data distributions. Our theoretical analysis underlines the robustness of CYBER-0, illustrating the limited ability of Byzantine clients to significantly influence the learning process. In future work, CYBER-0 can be further enhanced by exploring advanced compression techniques, such as quantization, to optimize the transmission of values within CYBER-0.

The importance of integrating privacy-enhancing measures further opens up many potential directions including the incorporation of differential privacy, homomorphic encryption, and secure multi-party computation. The inherent efficiency of CYBER-0 yields promising compatibility with privacy-preserving techniques, potentially opening up new frontiers in secure, private and efficient federated learning.

## References

- [1] B. McMahan, E. Moore, D. Ramage, S. Hampson, and B. A. y Arcas, “Communication-efficient learning of deep networks from decentralized data,” in *Artificial intelligence and statistics*, 2017, pp. 1273–1282.
- [2] Y. Zhao, M. Li, L. Lai, N. Suda, D. Civin, and V. Chandra, “Federated learning with non-iid data,” *arXiv preprint arXiv:1806.00582*, 2018.
- [3] H. Zhu, J. Xu, S. Liu, and Y. Jin, “Federated learning on non-iid data: A survey,” *Neurocomputing*, vol. 465, pp. 371–390, 2021.
- [4] R. Schlegel, S. Kumar, E. Rosnes, and A. G. i Amat, “Codedpaddedfl and codedsecagg: Straggler mitigation and secure aggregation in federated learning,” *IEEE Transactions on Communications*, 2023.
- [5] M. Egger, C. Hofmeister, A. Wachter-Zeh, and R. Bitar, “Private aggregation in wireless federated learning with heterogeneous clusters,” in *IEEE International Symposium on Information Theory (ISIT)*, 2023, pp. 54–59.
- [6] T. Jahani-Nezhad, M. A. Maddah-Ali, S. Li, and G. Caire, “Swiftagg+: Achieving asymptotically optimal communication loads in secure aggregation for federated learning,” *IEEE Journal on Selected Areas in Communications*, vol. 41, no. 4, pp. 977–989, 2023.
- [7] T. Zhu and S. Y. Philip, “Applying differential privacy mechanism in artificial intelligence,” in *IEEE International Conference on Distributed Computing Systems (ICDCS)*, 2019, pp. 1601–1609.
- [8] S. Truex, N. Baracaldo, A. Anwar, *et al.*, “A hybrid approach to privacy-preserving federated learning,” in *ACM workshop on artificial intelligence and security*, 2019, pp. 1–11.
- [9] E. Bagdasaryan, O. Poursaeed, and V. Shmatikov, “Differential privacy has disparate impact on model accuracy,” *Advances in neural information processing systems*, vol. 32, 2019.
- [10] K. Wei, J. Li, M. Ding, *et al.*, “Federated learning with differential privacy: Algorithms and performance analysis,” *IEEE Transactions on Information Forensics and Security*, vol. 15, pp. 3454–3469, 2020.
- [11] X. Tang, A. Panda, M. Nasr, S. Mahlouljifar, and P. Mittal, “Private fine-tuning of large language models with zeroth-order optimization,” *arXiv preprint arXiv:2401.04343*, 2024.
- [12] S. Shen, S. Tople, and P. Saxena, “Auror: Defending against poisoning attacks in collaborative deep learning systems,” in *Annual Conference on Computer Security Applications*, 2016, pp. 508–519.
- [13] P. Blanchard, E. M. El Mhamdi, R. Guerraoui, and J. Stainer, “Machine learning with adversaries: Byzantine tolerant gradient descent,” in *Advances in Neural Information Processing Systems*, vol. 30, 2017.
- [14] S. Li, Y. Cheng, W. Wang, Y. Liu, and T. Chen, “Learning to detect malicious clients for robust federated learning,” *arXiv preprint arXiv:2002.00211*, 2020.
- [15] D. Yin, Y. Chen, R. Kannan, and P. Bartlett, “Byzantine-robust distributed learning: Towards optimal statistical rates,” in *International Conference on Machine Learning*, 2018, pp. 5650–5659.

- [16] M. Xhemrishi, J. Östman, A. Wachter-Zeh, *et al.*, “Balancing privacy and security in federated learning with fedgt: A group testing framework,” *arXiv preprint arXiv:2305.05506*, 2023.
- [17] W. Wen, C. Xu, F. Yan, *et al.*, “Terngrad: Ternary gradients to reduce communication in distributed deep learning,” *Advances in neural information processing systems*, vol. 30, 2017.
- [18] S. P. Karimireddy, Q. Rebjock, S. Stich, and M. Jaggi, “Error feedback fixes SignSGD and other gradient compression schemes,” in *International Conference on Machine Learning*, 2019, pp. 3252–3261.
- [19] T. Vogels, S. P. Karimireddy, and M. Jaggi, “Powersgd: Practical low-rank gradient compression for distributed optimization,” *Advances in Neural Information Processing Systems*, vol. 32, 2019.
- [20] A. M. Abdelmoniem, A. Elzanaty, M.-S. Alouini, and M. Canini, “An efficient statistical-based gradient compression technique for distributed training systems,” *Proceedings of Machine Learning and Systems*, vol. 3, pp. 297–322, 2021.
- [21] A. V. Makkuva, M. Bondaschi, T. Vogels, M. Jaggi, H. Kim, and M. C. Gastpar, “Laser: Linear compression in wireless distributed optimization,” *arXiv preprint arXiv:2310.13033*, 2023.
- [22] Z. Tang, Y. Wang, and T.-H. Chang, “z-SignFedAvg: A unified stochastic sign-based compression for federated learning,” *arXiv preprint arXiv:2302.02589*, 2023.
- [23] Z. Qin, D. Chen, B. Qian, B. Ding, Y. Li, and S. Deng, “Federated full-parameter tuning of billion-sized language models with communication cost under 18 kilobytes,” *arXiv preprint arXiv:2312.06353*, 2023.
- [24] T. Salimans, J. Ho, X. Chen, S. Sidor, and I. Sutskever, “Evolution strategies as a scalable alternative to reinforcement learning,” *arXiv preprint arXiv:1703.03864*, 2017.
- [25] A. Ilyas, L. Engstrom, A. Athalye, and J. Lin, “Black-box adversarial attacks with limited queries and information,” in *International conference on machine learning*, 2018, pp. 2137–2146.
- [26] M. Malladi, T. Gao, E. Nichani, *et al.*, “Fine-tuning language models with just forward passes,” in *Conference on Neural Information Processing Systems*, 2023.
- [27] W. Fang, Z. Yu, Y. Jiang, Y. Shi, C. N. Jones, and Y. Zhou, “Communication-efficient stochastic zeroth-order optimization for federated learning,” *IEEE Transactions on Signal Processing*, vol. 70, pp. 5058–5073, 2022. (visited on 11/30/2023).
- [28] W. Fang, Z. Yu, Y. Jiang, Y. Shi, C. N. Jones, and Y. Zhou, “Communication-efficient stochastic zeroth-order optimization for federated learning,” *IEEE Transactions on Signal Processing*, vol. 70, pp. 5058–5073, 2022.
- [29] S. J. Wright, “Coordinate descent algorithms,” *Mathematical programming*, vol. 151, no. 1, pp. 3–34, 2015.
- [30] Y. Dong, X. Chen, K. Li, D. Wang, and S. Zeng, “Flod: Oblivious defender for private byzantine-robust federated learning with dishonest-majority,” in *European Symposium on Research in Computer Security*, Springer, 2021, pp. 497–518.
- [31] Z. Lu, S. Lu, X. Tang, and J. Wu, “Robust and verifiable privacy federated learning,” *IEEE Transactions on Artificial Intelligence*, 2023.
- [32] Y. Xia, C. Hofmeister, M. Egger, and R. Bitar, “Byzantine-resilient secure aggregation for federated learning without privacy compromises,” *arXiv preprint arXiv:2405.08698*, 2024.
- [33] Y. LeCun, L. Bottou, Y. Bengio, and P. Haffner, “Gradient-based learning applied to document recognition,” *Proceedings of the IEEE*, vol. 86, no. 11, pp. 2278–2324, 1998.
- [34] M. Fang, X. Cao, J. Jia, and N. Gong, “Local model poisoning attacks to byzantine-robust federated learning,” in *USENIX security symposium*, 2020, pp. 1605–1622.
- [35] Y. Liu, M. Ott, N. Goyal, *et al.*, “Roberta: A robustly optimized bert pretraining approach,” *arXiv preprint arXiv:1907.11692*, 2019.
- [36] R. Socher, A. Perelygin, J. Wu, *et al.*, “Recursive deep models for semantic compositionality over a sentiment treebank,” in *Conference on empirical methods in natural language processing*, 2013, pp. 1631–1642.
- [37] S. R. Bowman, G. Angeli, C. Potts, and C. D. Manning, “A large annotated corpus for learning natural language inference,” in *Empirical Methods in Natural Language Processing*, 2015, pp. 632–642.

- [38] E. M. Voorhees and D. M. Tice, “Building a question answering test collection,” in *Annual international ACM SIGIR conference on Research and development in information retrieval*, 2000, pp. 200–207.
- [39] T. Brown, B. Mann, N. Ryder, *et al.*, “Language models are few-shot learners,” *Advances in neural information processing systems*, vol. 33, pp. 1877–1901, 2020.
- [40] Y. Nesterov and V. Spokoiny, “Random Gradient-Free Minimization of Convex Functions,” *Foundations of Computational Mathematics*, vol. 17, no. 2, pp. 527–566, Apr. 2017.
- [41] X. Gao, B. Jiang, and S. Zhang, “On the information-adaptive variants of the admm: An iteration complexity perspective,” *Journal of Scientific Computing*, vol. 76, pp. 327–363, 2018.
- [42] M. Andriushchenko, F. Croce, N. Flammarion, and M. Hein, “Square attack: A query-efficient black-box adversarial attack via random search,” in *European conference on computer vision*, Springer, 2020, pp. 484–501.
- [43] M. A. Abdullah, H. Ren, H. B. Ammar, *et al.*, “Wasserstein robust reinforcement learning,” *arXiv preprint arXiv:1907.13196*, 2019.
- [44] F. Seide, H. Fu, J. Droppo, G. Li, and D. Yu, “1-bit stochastic gradient descent and its application to data-parallel distributed training of speech dnns,” in *Conference of the international speech communication association*, 2014.
- [45] J. Bernstein, Y.-X. Wang, K. Azizzadenesheli, and A. Anandkumar, “Signsgd: Compressed optimisation for non-convex problems,” in *International Conference on Machine Learning*, 2018, pp. 560–569.
- [46] E. Zelikman, Q. Huang, P. Liang, N. Haber, and N. D. Goodman, “Just one byte (per gradient): A note on low-bandwidth decentralized language model finetuning using shared randomness,” *arXiv preprint arXiv:2306.10015*, 2023.
- [47] A. R. Elkordy, S. Prakash, and S. Avestimehr, “Basil: A fast and byzantine-resilient approach for decentralized training,” *IEEE Journal on Selected Areas in Communications*, vol. 40, no. 9, pp. 2694–2716, 2022.
- [48] J. Xu, S.-L. Huang, L. Song, and T. Lan, “Byzantine-robust federated learning through collaborative malicious gradient filtering,” in *International Conference on Distributed Computing Systems (ICDCS)*, 2022, pp. 1223–1235.
- [49] C. Fung, C. J. Yoon, and I. Beschastnikh, “Mitigating sybils in federated learning poisoning,” *arXiv preprint arXiv:1808.04866*, 2018.
- [50] V. Tolpegin, S. Truex, M. E. Gursoy, and L. Liu, “Data poisoning attacks against federated learning systems,” in *European Symposium on Research in Computer Security (ESORICS)*, Springer, 2020, pp. 480–501.
- [51] R. Vershynin, “Introduction to the non-asymptotic analysis of random matrices,” *arXiv preprint arXiv:1011.3027*, 2010.
- [52] S. Bubeck *et al.*, “Convex optimization: Algorithms and complexity,” *Foundations and Trends® in Machine Learning*, vol. 8, no. 3-4, pp. 231–357, 2015.

## A Experiments

### A.1 Experimental Algorithm

In this appendix, we elaborate on the algorithm utilized for the experiments presented in Section 4. Algorithm 2 illustrates the optimization steps that enable CYBER-0 to attain both communication and memory efficiency. Notably, the key differences from Algorithm 1 include:

**Perturbation Direction Sampling.** Contrary to the original method of sampling the perturbation directions  $z$  from the unit sphere  $\mathbb{S}^d$  and scaling the estimate by a factor of  $d$ , our practical approach, similar to [24], [26] involves sampling each coordinate of  $z$  independently from a standard Gaussian distribution. This modification, while seemingly minor, has significant practical implications. On one hand, this modification retains our theoretical guarantees – the expected norm squared is identical to that of sampling over the unit sphere, and the normalized variance of the norm also decreases with increasing  $d$ . At the same time, from a practical point of view, it facilitates iterative sampling for each gradient coordinate, thereby considerably reducing the memory requirement in contrast to allocating the entire vector.

**Shared Randomness.** Since zero-order optimization requires clients and the federator to agree upon the perturbation directions, one approach would be that, each client receives the transmission of perturbation directions from the federator. This would entail a significant downlink communication overhead. Instead, our optimized method relies on pseudorandom generation. A single seed value is transmitted from the federator to the clients at the start of the training loop. This enables every client to independently reconstruct all perturbation directions, dismissing the need for direct transmission from the server. The principal advantage of this strategy lies in its significant reduction of communication costs per training step—from communicating a  $d$ -dimensional vector to merely a single value per sample.

**In-Place Operations.** The standard procedure involves allocating memory for intermediate values such as perturbation vectors and perturbed models. In our approach, again similar to [26], these operations are executed in place. This method not only conserves memory but also streamlines the computational process. By performing and subsequently reversing these operations in place, we manage to maintain a low memory footprint throughout the training phase.

---

**Algorithm 2** CYBER-0- Experimental Setup

---

**Input:**  $w^0$  is the initial model parameter vector,  $\beta$  is the trimmed mean factor,  $\eta$  is the learning rate,  $\mu$  is the perturbation step,  $k$  is the number of samples per estimate and  $T$  is the total number of learning steps.

► **Federator**

Distributes a random seed  $s$  to each client  
Distributes  $w_i^0 = w^0$  to each client

**for**  $t = 0$  **to**  $T$  **do**

**for**  $i = 1$  **to**  $m$  **in parallel do**

    ▷ **client**  $i$

**for**  $r = 1$  **to**  $k$  **do**

$s' \leftarrow (s, t, r)$

$g_r^i \leftarrow \begin{cases} \text{ZOGRAD}(F, w_i^t, B, \mu, s') & \text{if } i \notin \mathcal{B} \\ * & \text{else} \end{cases}$

**end for**

      Sends  $\{g_r^i\}_{r=1}^k$  to federator

**end for**

// Federator robust aggregation

► **Federator**

**for**  $r = 1$  **to**  $k$  **do**

$\hat{g}_r \leftarrow \text{trmean}_\beta \{ \{g_r^i\}_{i=1}^m \}$

$w^t \leftarrow \text{PERTURBPARAMS}(w^t, -\frac{\eta \hat{g}_r}{k}, s')$

**end for**

  Sends  $\{ \{\hat{g}_r\}_{r=1}^k \}$  to each client

// clients synchronization

**for**  $i = 1$  **to**  $m$  **in parallel do**

  ▷ **client**  $i$

**for**  $r = 1$  **to**  $k$  **do**

$s' \leftarrow (s, t, r)$

$w_i^t \leftarrow \text{PERTURBPARAMS}(w_i^t, -\frac{\eta \hat{g}_r}{k}, s')$

**end for**

**end for**

**end for**

**function** ZOGRAD( $F, w, B, \mu, s'$ )

$w \leftarrow \text{PERTURBPARAMS}(w, \mu, s')$

$l_+ \leftarrow F(w, B)$

$w \leftarrow \text{PERTURBPARAMS}(w, -2\mu, s')$

$l_- \leftarrow F(w, B)$

```

 $\mathbf{w} \leftarrow \text{PERTURBPARAMS}(\mathbf{w}, \mu, s')$  // Reset model state
Return  $\frac{l_+ - L_-}{2\mu}$ 
end function

function PERTURBPARAMS( $\mathbf{w}, \mu, s'$ )
  Set RNG seed as  $s'$ 
  for each  $\mathbf{w}^{(i)}$  in  $\mathbf{w}$  do
     $z \sim \mathcal{N}(0, 1)$ 
     $\mathbf{w}^{(i)} \leftarrow \mathbf{w}^{(i)} + \mu z$  // Memory efficient
  end for
end function

```

---

We provide here the Algorithm summarizing the Full-Knowledge attack.

---

**Algorithm 3** Full-Knowledge Byzantine Behavior

---

```

Input:  $\mathbf{w}^t, \beta, \mu, \mathbf{z}_r^t, g_i(\mathbf{w}^t, \mathbf{z}_r^t) \forall i \in [m]$ .
for device  $b \in \mathcal{B}$  do
   $\hat{g}_{true} \leftarrow \frac{1}{m} \sum_{i=1}^m g_i(\mathbf{w}^t, \mathbf{z}_r^t)$ 
  if  $\hat{g}_{true} \geq 0$  then
    Send the  $\lfloor \beta m \rfloor$ -th smallest value of  $\{g_i(\mathbf{w}^t, \mathbf{z}_r^t) : i \in [m] \setminus \mathcal{B}\}$ 
  else
    Send the  $\lfloor \beta m \rfloor$ -th largest value of  $\{g_i(\mathbf{w}^t, \mathbf{z}_r^t) : i \in [m] \setminus \mathcal{B}\}$ 
  end if
end for

```

---

## A.2 Simulation Parameters and Hyperparameters

### A.2.1 Logistic Regression on MNIST

The simulation parameters and hyperparameters for all CYBER-0 experiments in Section 4.2 are found in Table 4. Exceptionally, in the experiments of Table 1, we use  $m = 40$ , to reproduce the same settings as in [15]. All results in Section 4.2 are averaged across three random seeds.

Table 4: Simulation Parameters and Hyperparameters for Section 4.2

We run all of our simulations in a single GPU setting using an Nvidia RTX 4090 GPU.

MNIST DATA SET	
GLOBAL TRAIN SAMPLES	60,000
NUMBER OF CLIENTS	12
NUMBER OF BYZANTINE CLIENTS	3
$\beta$	0.25
LEARNING RATE	$10^{-2}$
CLIENT BATCH SIZE	64
LEARNING STEPS	400

### A.2.2 Prompt-Based Fine-Tuning

The simulation parameters and hyperparameters for all CYBER-0 experiments in Section 4.3 are found in Table 5. For Table 2 and 2, results are averaged across three different random seeds.

Table 5: Simulation Parameters and Hyperparameters for Section 4.3

	SST-2	SNLI	TREC
GLOBAL TRAIN SAMPLES	—	512	—
NUMBER OF CLIENTS	8	12	12
NUMBER OF BYZANTINE CLIENTS	2	3	3
$\beta$	—	0.25	—
LEARNING RATE	—	$10^{-6}$	—
CLIENT BATCH SIZE	—	64	—
LEARNING STEPS	20,000	20,000	40,000

## A.3 Further Loss Curves for TREC and SNLI

In this section, we present two additional loss curves for the TREC and SNLI experiments. Both curves are shown in Figure 3. For both datasets, we observe a convergence reduction for the Non-Byzantine setting. For SNLI, the reduction appears greater, which aligns with the results in Table 2.

## A.4 Local Epochs

In our experimental framework, we extended our investigation to evaluate the performance of CYBER-0 under the context of local epochs. This involved adapting our practical algorithm (Algorithm 2) to include local epochs, incorporating memory-efficient operations, as detailed in Algorithm 4.

Our findings, as summarized in Table 6, reveal an intriguing parallel to the impact of the variable  $k$ . Specifically, modifying the number of local epochs appears to exert a comparable influence. A notable insight from this experiment is the relative stability of the final test accuracy, despite variations in batching these training epochs. However, it’s important to acknowledge that the efficacy of such a technique can be highly dependent on the specific problem at hand, suggesting a need for cautious interpretation and application in different contexts.

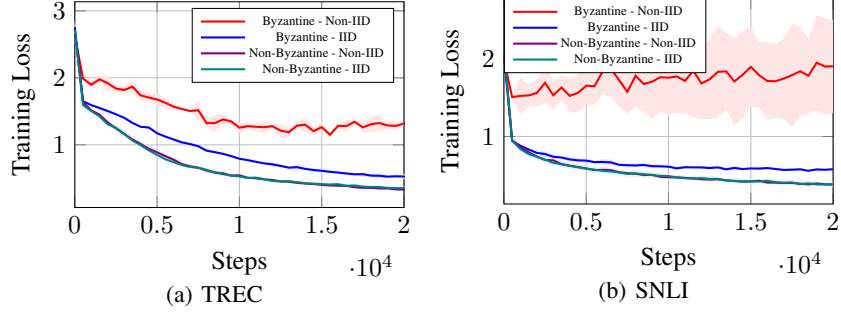


Figure 3: Contrasting Byzantine and Non-Byzantine Scenarios Across Diverse Data Distributions with RoBERTa-large on TREC and SNLI: This figure compares the performance of CYBER-0 using a RoBERTa-large model on both TREC and SNLI datasets. Non-Byzantine behavior stands for CYBER-0 with no Byzantine clients nor robust aggregation.

Table 6: Assessing the Impact of Varying Local Epochs in SST-2 Using RoBERTa-large: This table provides a comparative analysis of how different settings for local epochs affect performance on the SST-2 dataset using the RoBERTa-large model on a Byzantine and non-IID setting.

LOCAL EPOCHS	COMMUNICATION ROUNDS	TEST ACCURACY
1	20,000	92.7 ± 0.4
5	4,000	92.6 ± 0.3
50	400	92.8 ± 0.5
100	200	92.4 ± 0.2

---

**Algorithm 4** CYBER-0- Experimental Setup with Local Epochs

---

**Input:**  $w^0$  is the initial model parameter vector,  $\beta$  is the trimmed mean factor,  $\eta$  is the learning rate,  $\mu$  is the perturbation step,  $k$  is the number of samples per estimate,  $E$  is the number of local epochs and  $T$  is the total number of learning steps.

► **Federator**

Distributes a random seed  $s$  to each client

Distributes  $w_i = w^0$  to each client

Sets  $w \leftarrow w^0$

**for**  $t = 1$  **to**  $T$  **do**

**for**  $i = 1$  **to**  $m$  **in parallel do**

    ▷ **client**  $i$

**for**  $e = 1$  **to**  $E$  **do**

        // Sample  $k$  grad estimates

**for**  $r = 1$  **to**  $k$  **do**

$s' \leftarrow (s, t, r, e)$

$g_{r,e}^{i,t} \leftarrow \begin{cases} \text{ZOGRAD}(F, w_i, B, \mu, s') & \text{if } i \notin \mathcal{B} \\ * & \text{else} \end{cases}$

**end for**

        // Apply local epoch learning step

**for**  $r = 1$  **to**  $k$  **do**

$s' \leftarrow (s, t, r, e)$

$w_i \leftarrow \text{PERTURBPARAMS}(w_i, -\frac{\eta g_{r,e}^{i,t}}{k}, s')$

**end for**

**end for**

      // Reset model to start of local epochs (alternatively, can store initial model, with extra memory cost)

**for**  $e = 1$  **to**  $E$  **do**



```

    for  $r = 1$  to  $k$  do
         $s' \leftarrow (s, t, r, e)$ 
         $w_i \leftarrow \text{PERTURBPARAMS}(w_i, \frac{\eta g_{r,e}^{i,t}}{k}, s')$ 
    end for
end for
Sends  $\left\{ \left\{ g_{r,e}^{i,t} \right\}_{r=1}^k \right\}_{e=1}^E$  to federator
end for

// Federator robust aggregation
► Federator
for  $e = 1$  to  $E$  do
    for  $r = 1$  to  $k$  do
         $\hat{g}_{r,e}^t \leftarrow \text{TrMn}_\beta \left\{ \left\{ g_{r,e}^i \right\}_{i=1}^m \right\}$ 
         $s' \leftarrow (s, t, r, e)$ 
         $w \leftarrow \text{PERTURBPARAMS}(w, -\frac{\eta \hat{g}_{r,e}^t}{k}, s')$ 
    end for
end for
Sends  $\left\{ \left\{ \hat{g}_{r,e}^t \right\}_{r=1}^k \right\}_{e=1}^E$  to each client

// clients synchronization
for  $i = 1$  to  $m$  in parallel do
    ▷ client  $i$ 
    for  $e = 1$  to  $E$  do
        for  $r = 1$  to  $k$  do
             $s' \leftarrow (s, t, r, e)$ 
             $w_i \leftarrow \text{PERTURBPARAMS}(w_i, -\frac{\eta \hat{g}_{r,e}^t}{k}, s')$ 
        end for
    end for
end for
end for

function ZOGRAD( $F, w, B, \mu, s'$ )
     $w \leftarrow \text{PERTURBPARAMS}(w, \mu, s')$ 
     $l_+ \leftarrow F(w, B)$ 
     $w \leftarrow \text{PERTURBPARAMS}(w, -2\mu, s')$ 
     $l_- \leftarrow F(w, B)$ 
     $w \leftarrow \text{PERTURBPARAMS}(w, \mu, s')$  // Reset model state
    Return  $\frac{l_+ - l_-}{2\mu}$ 
end function

function PERTURBPARAMS( $w, \mu, s'$ )
    Set RNG seed as  $s'$ 
    for each  $w^{(i)}$  in  $w$  do
         $z \sim \mathcal{N}(0, 1)$ 
         $w^{(i)} \leftarrow w^{(i)} + \mu z$  // Memory efficient
    end for
end function

```

---

## B Proofs

In this appendix we derive the proofs for the Theorems in Section 5.

### B.1 Proof of Theorem 5.8

In proving Theorem 5.8, we begin by invoking a lemma from [15]. This lemma provides a probabilistic upper bound for the maximum deviation in a one-dimensional robust mean estimation problem of a random variable, within the context of our client setup described in Section 2.

**Lemma B.1.** (Lemma 3, [15]) *Let  $x$  be a  $v$ -sub-exponential random variable with mean  $\mu_x$ . For all  $i \in [m]$  and  $j \in [n]$  Let  $x^{i,j}$  is the  $j$ -th sample of  $x$  in client  $i$  if the client is benign or arbitrary adversarial data otherwise, and let  $\bar{x}^i = \frac{1}{n} \sum_{j=1}^n x^{i,j}$ . Then, for any  $t > 0$ , Byzantine fraction  $0 \leq \alpha < \frac{1}{2}$  and trimmed mean factor  $\beta$ .*

$$P \left\{ \left| \frac{1}{(1-\alpha)m} \sum_{i \in [m] \setminus \mathcal{B}} \bar{x}^i - \mu_x \right| \geq t \right\} \leq 2 \exp \left\{ -(1-\alpha)mn \min \left\{ \frac{t}{2v}, \frac{t^2}{2v^2} \right\} \right\},$$

for any  $s > 0$

$$P \left\{ \max_{i \in [m] \setminus \mathcal{B}} \{ |\bar{x}^i - \mu_x| \} \geq s \right\} \leq 2(1-\alpha)m \exp \left\{ -n \min \left\{ \frac{s}{2v}, \frac{s^2}{2v^2} \right\} \right\},$$

and when  $\beta \geq \alpha$ ,  $\left| \frac{1}{(1-\alpha)m} \sum_{i \in [m] \setminus \mathcal{B}} \bar{x}^i - \mu_x \right| \leq t$ , and  $\max_{i \in [m] \setminus \mathcal{B}} \{ |\bar{x}^i - \mu_x| \} \leq s$

$$|\text{TrMn}_\beta \{ \bar{x}^i : i \in [m] \} - \mu_x| \leq \frac{t + 3\beta s}{1 - 2\beta}.$$

With Lemma B.1 as our foundation, we proceed to prove Theorem 5.8 by applying it to the norm of the client estimate  $g_i(\mathbf{w}, \mathbf{z})$ . For  $s, t, \mu \geq 0$  and  $\mathbf{z} \in \mathbb{S}^d$ , we can state that with no smaller probability than

$$1 - 2 \exp \left\{ -(1-\alpha)mn \min \left\{ \frac{t}{2v}, \frac{t^2}{2v^2} \right\} \right\} - 2(1-\alpha)m \exp \left\{ -n \min \left\{ \frac{s}{2v}, \frac{s^2}{2v^2} \right\} \right\},$$

the trimmed mean of client estimates is bounded as

$$|\hat{g}_\beta(\mathbf{w}, \mathbf{z}) - \bar{g}(\mathbf{w}, \mathbf{z})| = |\text{TrMn}_\beta \{ g_i(\mathbf{w}, \mathbf{z}) : i \in [m] \} - \bar{g}(\mathbf{w}, \mathbf{z})| \leq \frac{t + 3\beta s}{1 - 2\beta}.$$

To extend this result to all  $\mathbf{w} \in \mathcal{W}$  and any  $k$  samples of vectors  $\mathbf{z}_r$ , we follow the methodology outlined in [15], utilizing a covering set argument on both  $\mathcal{W}$  and  $\mathbb{S}^d$ . We define  $W_\delta = \{ \mathbf{w}^1, \mathbf{w}^2, \dots, \mathbf{w}^{N_\delta} \}$  and  $Z_\delta = \{ \mathbf{z}^1, \mathbf{z}^2, \dots, \mathbf{z}^{M_\delta} \}$ , where  $N_\delta, M_\delta \in \mathbb{N}$ , such that for all  $\mathbf{w} \in \mathcal{W}$  and  $\mathbf{z} \in \mathbb{S}^d$ , there exists an  $l \in [N_\delta]$  and  $q \in [M_\delta]$  such that  $\|\mathbf{w}^l - \mathbf{w}\|_2 \leq \delta$  and  $\|\mathbf{z}^q - \mathbf{z}\|_2 \leq \delta$ . According to [51], it is always possible to find such sets satisfying  $N_\delta \leq (1 + \frac{D}{\delta})^d$  and  $M_\delta \leq (1 + \frac{2}{\delta})^d$ .

Applying the union bound, with probabilities at least  $1 - 2M_\delta N_\delta \exp \left\{ -(1-\alpha)mn \min \left\{ \frac{t}{2v}, \frac{t^2}{2v^2} \right\} \right\}$  and  $1 - 2M_\delta N_\delta (1-\alpha)m \exp \left\{ -n \min \left\{ \frac{s}{2v}, \frac{s^2}{2v^2} \right\} \right\}$ , we can ensure that  $\left| \frac{1}{(1-\alpha)m} \sum_{i \in [m] \setminus \mathcal{B}} g_i(\mathbf{w}^l, \mathbf{z}^q) - \bar{g}(\mathbf{w}^l, \mathbf{z}^q) \right| \leq t$  and  $\max_{i \in [m] \setminus \mathcal{B}} \{ |g_i(\mathbf{w}^l, \mathbf{z}^q) - \bar{g}(\mathbf{w}^l, \mathbf{z}^q)| \} \leq s$ , respectively, for all  $\mathbf{w}^l \in W_\delta$  and  $\mathbf{z}^q \in Z_\delta$ .

In the event of these joint conditions being met, we have

$$|\hat{g}_\beta(\mathbf{w}^l, \mathbf{z}^q) - \bar{g}(\mathbf{w}^l, \mathbf{z}^q)| \leq \frac{t + 3\beta s}{1 - 2\beta}$$

for all  $\mathbf{w}^l \in W_\delta$  and  $\mathbf{z}^q \in Z_\delta$ .

Now, using both the  $L_{w,\mu}$ -Lipschitz property of  $g(\cdot, z, \gamma)$  and the  $L_{z,\mu}$ -Lipschitz property of  $g(\mathbf{w}, \cdot, \gamma)$  for any data sample  $\gamma$  from Assumption 5.5, and the fact that for all  $\mathbf{w} \in \mathcal{W}$  and  $\mathbf{z} \in \mathbb{S}^d$ , there exists  $\mathbf{w}^l \in W_\delta$  and  $\mathbf{z}^q \in Z_\delta$  such that  $\|\mathbf{w}^l - \mathbf{w}\|_2 \leq \delta$  and  $\|\mathbf{z}^q - \mathbf{z}\|_2 \leq \delta$ , we have that for any benign client  $i$ ,  $|g_i(\mathbf{w}^l, \mathbf{z}^q) - g_i(\mathbf{w}, \mathbf{z})| \leq (L_{w,\mu} + L_{z,\mu})\delta$  and  $|\bar{g}(\mathbf{w}^l, \mathbf{z}^q) - \bar{g}(\mathbf{w}, \mathbf{z})| \leq (L_{w,\mu} + L_{z,\mu})\delta$ .

So first, in the event of  $|\frac{1}{(1-\alpha)m} \sum_{i \in [m] \setminus \mathcal{B}} g_i(\mathbf{w}^l, \mathbf{z}^q) - \bar{g}(\mathbf{w}^l, \mathbf{z}^q)| \leq t$  for all  $\mathbf{w}^l \in W_\delta$  and  $\mathbf{z} \in Z_\delta$  and by making use of the triangle inequality, we have for all  $\mathbf{w} \in \mathcal{W}$  and  $\mathbf{z} \in \mathbb{S}^d$

$$\begin{aligned} \left| \frac{1}{(1-\alpha)m} \sum_{i \in [m] \setminus \mathcal{B}} g_i(\mathbf{w}, \mathbf{z}) - \bar{g}(\mathbf{w}, \mathbf{z}) \right| &\leq \left| \frac{1}{(1-\alpha)m} \sum_{i \in [m] \setminus \mathcal{B}} g_i(\mathbf{w}^l, \mathbf{z}^q) - \bar{g}(\mathbf{w}^l, \mathbf{z}^q) \right| \\ &\quad + \frac{1}{(1-\alpha)m} \sum_{i \in [m] \setminus \mathcal{B}} |g_i(\mathbf{w}^l, \mathbf{z}^q) - g_i(\mathbf{w}, \mathbf{z})| + |\bar{g}(\mathbf{w}^l, \mathbf{z}^q) - \bar{g}(\mathbf{w}, \mathbf{z})| \\ &\leq t + 2(L_{w,\mu} + L_{z,\mu})\delta, \end{aligned}$$

and similarly, having  $\max_{i \in [m] \setminus \mathcal{B}} \{|g_i(\mathbf{w}^l, \mathbf{z}^q) - \bar{g}(\mathbf{w}^l, \mathbf{z}^q)|\} \leq s$  for all  $\mathbf{w}^l \in W_\delta$  and  $\mathbf{z} \in Z_\delta$  implies that

$$\max_{i \in [m] \setminus \mathcal{B}} \{|g_i(\mathbf{w}, \mathbf{z}) - \bar{g}(\mathbf{w}, \mathbf{z})|\} \leq s + 2(L_{w,\mu} + L_{z,\mu})\delta$$

further implying

$$\|\hat{g}_\beta(\mathbf{w}, \mathbf{z}) - \bar{\mathbf{g}}(\mathbf{w}, \mathbf{z})\|_2 = |\text{TrMn}_\beta \{g_i(\mathbf{w}, \mathbf{z}) : i \in [m]\} - \bar{g}(\mathbf{w}, \mathbf{z})| \leq \frac{t + 3\beta s}{1 - 2\beta} + \frac{2(1 + 3\beta)}{1 - 2\beta} \delta (L_{w,\mu} + L_{z,\mu})$$

which leads us, by applying the triangle inequality, to the final bound

$$\left\| \frac{1}{k} \sum_{r=1}^k \hat{g}_\beta(\mathbf{w}, \mathbf{z}_r) - \frac{1}{k} \sum_{r=1}^k \bar{\mathbf{g}}(\mathbf{w}, \mathbf{z}_r) \right\|_2 \leq \frac{t + 3\beta s}{1 - 2\beta} + \frac{2(1 + 3\beta)}{1 - 2\beta} \delta \hat{L}_\mu$$

for  $\hat{L}_\mu = L_{w,\mu} + L_{z,\mu}$ .

Choosing  $\delta = \frac{1}{nm\hat{L}_\mu}$ ,

$$t = v \max \left\{ \frac{8d}{nm} \log [(1 + nm\hat{L}_\mu D)(1 + 2nm\hat{L}_\mu)], \sqrt{\frac{8d}{nm} \log [(1 + nm\hat{L}_\mu D)(1 + 2nm\hat{L}_\mu)]} \right\},$$

and

$$s = v \max \left\{ \frac{4}{n} (d \log [(1 + nm\hat{L}_\mu D)(1 + 2nm\hat{L}_\mu)] + \log m), \sqrt{\frac{4}{n} (d \log [(1 + nm\hat{L}_\mu D)(1 + 2nm\hat{L}_\mu)] + \log m)} \right\}$$

completes the proof.  $\square$

## B.2 Proof of Theorem 5.10

In order to prove Theorem 5.10 we instantiate several lemmas on the probabilistic behavior of the function  $\bar{\mathbf{g}}(\mathbf{w}, \mathbf{z})$  for the case  $\mu = 0$ .

**Lemma B.2.** (Lemma 7.3 (b) [41])  $\mathbb{E}_{\mathbf{z} \sim \mathbb{S}^d} [\mathbf{z}\mathbf{z}^\top] = \frac{1}{d}I_d$ , where  $I_d$  is the  $d$ -dimensional identity matrix.

**Lemma B.3.** The following holds.

$$\mathbb{E}_{\mathbf{z}_1, \mathbf{z}_2 \sim \mathbb{S}^d} [\mathbf{z}_1 \mathbf{z}_1^\top \mathbf{z}_2 \mathbf{z}_2^\top] = \begin{cases} \frac{1}{d}I_d, & \text{if } \mathbf{z}_1 = \mathbf{z}_2, \\ \frac{1}{d^2}I_d, & \text{if } \mathbf{z}_1 \text{ and } \mathbf{z}_2 \text{ are independent.} \end{cases}$$

*Proof.* In the case  $z_1 = z_2$ ,

$$\begin{aligned}\mathbb{E}_{z_1, z_2 \sim \mathbb{S}^d} [z_1 z_1^\top z_2 z_2^\top] &= \mathbb{E}_{z_1 \sim \mathbb{S}^d} [z_1 z_1^\top z_1 z_1^\top] \\ &= \mathbb{E}_{z_1 \sim \mathbb{S}^d} [z_1 z_1^\top]\end{aligned}$$

and the result is given by Lemma B.2.

In the case that  $z_1$  and  $z_2$  are independent,

$$\mathbb{E}_{z_1, z_2 \sim \mathbb{S}^d} [z_1 z_1^\top z_2 z_2^\top] = \mathbb{E}_{z_1 \sim \mathbb{S}^d} [z_1 z_1^\top] \mathbb{E}_{z_2 \sim \mathbb{S}^d} [z_2 z_2^\top]$$

And again, by Lemma B.2, the result is yielded.  $\square$

**Lemma B.4.** Let  $w \in \mathbb{R}^d$ ,

$$\mathbb{E}_{z \sim \mathbb{S}^d} [\bar{\mathbf{g}}(w, z, 0)] = \nabla F(w).$$

*Proof.*

$$\begin{aligned}\mathbb{E}_{z \sim \mathbb{S}^d} [\bar{\mathbf{g}}(w, z, 0)] &= \mathbb{E}_{z \sim \mathbb{S}^d} [d \langle \nabla F(w), z \rangle z] \\ &= d \mathbb{E}_{z \sim \mathbb{S}^d} [z z^\top] \nabla F(w) \\ &= \nabla F(w)\end{aligned}$$

where the last equality comes from Lemma B.2  $\square$

**Lemma B.5.** Let  $w \in \mathbb{R}^d$  and  $z_r$  independently sampled from  $\mathbb{S}^d$ ,  $r \in [k]$ ,

$$\mathbb{E}_{z_r \sim \mathbb{S}^d} \left[ \left\| \frac{1}{k} \sum_{r=1}^k \bar{\mathbf{g}}(w, z_r, 0) \right\|_2^2 \right] = \frac{d+k-1}{k} \|\nabla F(w)\|_2^2.$$

*Proof.*

$$\begin{aligned}\mathbb{E}_{z_r \sim \mathbb{S}^d} \left[ \left\| \frac{1}{k} \sum_{r=1}^k \bar{\mathbf{g}}(w, z_r, 0) \right\|_2^2 \right] &= \mathbb{E}_{z_r \sim \mathbb{S}^d} \left[ \left\| \frac{d}{k} \sum_{r=1}^k \nabla F(w)^\top z_r z_r \right\|_2^2 \right] \\ &= \frac{d^2}{k^2} \sum_{r=1}^k \sum_{s=1}^k \nabla F(w)^\top \mathbb{E}_{z_r, z_s \sim \mathbb{S}^d} [z_r z_r^\top z_s z_s^\top] \nabla F(w) \\ &= \frac{d^2}{k^2} \left( \frac{k}{d} + \frac{k(k-1)}{d^2} \right) \|\nabla F(w)\|_2^2\end{aligned}$$

where the last equality comes from B.3.  $\square$

**Lemma B.6.** (Co-coercivity of strongly convex functions, Lemma 3.11 [52]) Let  $F$  be  $L_F$ -smooth and  $\lambda$ -strongly convex. For all  $w_1, w_2 \in \mathbb{R}^d$

$$(\nabla F(w_1) - \nabla F(w_2))^\top (w_1 - w_2) \geq \frac{\lambda L_F}{\lambda + L_F} \|w_1 - w_2\|_2^2 + \frac{1}{\lambda + L_F} \|\nabla F(w_1) - \nabla F(w_2)\|_2^2.$$

With these lemmas in hand, we can proceed to prove Theorem 5.10. Let's consider the  $t$ -th step of Algorithm 1, then for  $\Pi_{\mathcal{W}}$  denoting the euclidean projection over  $\mathcal{W}$ , we have

$$\begin{aligned}\|w^{t+1} - w^*\|_2 &= \left\| \Pi_{\mathcal{W}} \left( w^t - \eta \frac{1}{k} \sum_{r=1}^k \hat{g}_\beta(w, z_r^t, 0) z_r^t \right) - w^* \right\|_2 \\ &\stackrel{(i)}{\leq} \left\| w^t - \eta \frac{1}{k} \sum_{r=1}^k \hat{g}_\beta(w, z_r^t, 0) z_r^t - w^* \right\|_2 \\ &\leq \left\| w^t - \eta \frac{1}{k} \sum_{r=1}^k \bar{\mathbf{g}}(w, z_r^t, 0) - w^* \right\|_2 + \eta \left\| \frac{1}{k} \sum_{r=1}^k \hat{g}_\beta(w^t, z_r, 0) z_r - \frac{1}{k} \sum_{r=1}^k \bar{\mathbf{g}}(w^t, z_r, 0) \right\|_2 \\ &\stackrel{(ii)}{\leq} \left\| w^t - \eta \frac{1}{k} \sum_{r=1}^k \bar{\mathbf{g}}(w, z_r^t, 0) - w^* \right\|_2 + \eta \Delta\end{aligned}$$

where (i) comes from the properties of Euclidean projection and (ii) comes from conditioning on the event from Theorem 5.8.

Now, by taking the expectation over  $Z^t$ ,

$$\mathbb{E}_{Z^t} [\|\mathbf{w}^{t+1} - \mathbf{w}^*\|_2] \leq \underbrace{\mathbb{E}_{Z^t} \left[ \left\| \mathbf{w}^t - \eta \frac{1}{k} \sum_{r=1}^k \bar{\mathbf{g}}(\mathbf{w}, \mathbf{z}_r^t, 0) - \mathbf{w}^* \right\|_2 \right]}_{T_1} + \eta \Delta$$

We need to further bound the term  $T_1$ . We do that by considering

$$\begin{aligned} & \mathbb{E}_{Z^t} \left[ \left\| \mathbf{w}^t - \eta \frac{1}{k} \sum_{r=1}^k \bar{\mathbf{g}}(\mathbf{w}, \mathbf{z}_r^t, 0) - \mathbf{w}^* \right\|_2^2 \right] \\ &= \mathbb{E}_{Z^t} \left[ \|\mathbf{w}^t - \mathbf{w}^*\|_2^2 - 2\eta \left\langle \mathbf{w}^t - \mathbf{w}^*, \frac{1}{k} \sum_{r=1}^k \bar{\mathbf{g}}(\mathbf{w}, \mathbf{z}_r^t, 0) \right\rangle + \eta^2 \left\| \frac{1}{k} \sum_{r=1}^k \bar{\mathbf{g}}(\mathbf{w}, \mathbf{z}_r^t, 0) \right\|_2^2 \right] \\ &\stackrel{(i)}{=} \|\mathbf{w}^t - \mathbf{w}^*\|_2^2 - 2\eta \langle \mathbf{w}^t - \mathbf{w}^*, \nabla F(\mathbf{w}^t) \rangle + \eta^2 \frac{d+k-1}{k} \|\nabla F(\mathbf{w}^t)\|_2^2 \\ &\stackrel{(ii)}{\leq} \left( 1 - \frac{2\lambda k}{(d+k-1)(L_F + \lambda)} \right) \|\mathbf{w}^t - \mathbf{w}^*\|_2^2 - \left( \frac{2}{L_F(\lambda + L_F)} - \frac{1}{L_F^2} \right) \frac{k}{d+k-1} \|\nabla F(\mathbf{w}^t)\|_2^2 \\ &\stackrel{(iii)}{\leq} \left( 1 - \frac{2\lambda k}{(d+k-1)(L_F + \lambda)} \right) \|\mathbf{w}^t - \mathbf{w}^*\|_2^2 \end{aligned}$$

where (i) comes from Lemmas B.4 and B.5, (ii) comes from Lemma B.6, Assumption 5.3 and the choice of  $\eta = \frac{k}{L_F(d+k-1)}$  and (iii) comes from the fact that  $\lambda \leq L_F$ .

Then by applying Jensen's inequality on the square root function and using the fact that  $\sqrt{1-x} \leq 1 - \frac{x}{2}$ , we can bound  $T_1$  as

$$\mathbb{E}_{Z^t} \left[ \left\| \mathbf{w}^t - \eta \frac{1}{k} \sum_{r=1}^k \bar{\mathbf{g}}(\mathbf{w}, \mathbf{z}_r^t, 0) - \mathbf{w}^* \right\|_2 \right] \leq \left( 1 - \frac{\lambda k}{(d+k-1)(L_F + \lambda)} \right) \|\mathbf{w}^t - \mathbf{w}^*\|_2$$

Thus,

$$\mathbb{E}_{Z^t} [\|\mathbf{w}^{t+1} - \mathbf{w}^*\|_2] \leq \left( 1 - \frac{\lambda k}{(d+k-1)(L_F + \lambda)} \right) \|\mathbf{w}^t - \mathbf{w}^*\|_2 + \frac{k}{(d+k-1)L_F} \Delta$$

The proof is finished by taking the expectation over  $Z^{t-1}$  and recursively applying the inequality.

### B.3 Proof of Theorem 5.13

For Theorem 5.13 we need similar lemmas as we had for the proof of Theorem 5.10, in particular, we need the expected value of the zero-order estimate and a bound on its squared norm.

**Lemma B.7.** (Lemma 4.1 (a) [41]) Let  $\mathbf{w} \in \mathbb{R}^d$  and let  $F_\mu$  be as defined in Definition 5.11, then

$$\nabla F_\mu(\mathbf{w}) = \mathbb{E}_{\mathbf{z} \sim \mathbb{S}^d} \left[ \frac{d}{\mu} F(\mathbf{w} + \mu \mathbf{z}) \mathbf{z} \right].$$

**Lemma B.8.** Let  $\mathbf{w} \in \mathbb{R}^d$  and let  $F_\mu$  be as defined in Definition 5.11, then

$$\mathbb{E}_{\mathbf{z} \sim \mathbb{S}^d} [\bar{\mathbf{g}}(\mathbf{w}, \mathbf{z})] = \nabla F_\mu(\mathbf{w}).$$

*Proof.*

$$\begin{aligned}
\mathbb{E}_{\mathbf{z} \sim \mathbb{S}^d} [\bar{\mathbf{g}}(\mathbf{w}, \mathbf{z})] &= \frac{1}{2} \mathbb{E}_{\mathbf{z} \sim \mathbb{S}^d} \left[ \frac{d}{\mu} (F(\mathbf{w} + \mu\mathbf{z}) - F(\mathbf{w} - \mu\mathbf{z})) \mathbf{z} \right] \\
&= \frac{1}{2} \mathbb{E}_{\mathbf{z} \sim \mathbb{S}^d} \left[ \frac{d}{\mu} F(\mathbf{w} + \mu\mathbf{z}) \mathbf{z} \right] - \frac{1}{2} \mathbb{E}_{\mathbf{z} \sim \mathbb{S}^d} \left[ \frac{d}{\mu} F(\mathbf{w} - \mu\mathbf{z}) \mathbf{z} \right] \\
&= \mathbb{E}_{\mathbf{z} \sim \mathbb{S}^d} \left[ \frac{d}{\mu} F(\mathbf{w} + \mu\mathbf{z}) \mathbf{z} \right]
\end{aligned}$$

where the last equality comes from  $\mathbf{z}$  and  $-\mathbf{z}$  being identically distributed due to the symmetry of  $\mathbb{S}^d$ .  $\square$

**Lemma B.9.** (Equation (12) [40]) Let  $F_\mu$  be as defined in Definition 5.11. For any  $\mu > 0$ , if  $F$  is  $L_F$ -smooth, then  $F_\mu$  is  $L_F$ -smooth.

**Lemma B.10.** Let  $\mathbf{w} \in \mathbb{R}^d$  and let  $F_\mu$  be as defined in Definition 5.11, then

$$\|\nabla F(\mathbf{w})\|_2^2 \leq 2\|\nabla F_\mu(\mathbf{w})\|_2^2 + \frac{L_F^2 \mu^2 d^2}{2}.$$

*Proof.* From Lemma 4.1 (b) in [41], we know that  $\|\nabla F(\mathbf{w}) - \nabla F_\mu(\mathbf{w})\|_2 \leq \frac{L_F \mu d}{2}$ . The result follows from applying the triangle inequality and the fact that  $(x + y)^2 \leq \frac{x^2 + y^2}{2}$ .  $\square$

**Lemma B.11.** Let  $F_\mu$  be as defined in Definition 5.11. For any  $\mu > 0$ , if  $F$  is  $\lambda$ -strongly convex, then  $F_\mu$  is  $\lambda$ -strongly convex.

*Proof.* Let  $\mathbf{w}_1, \mathbf{w}_2 \in \mathbb{R}^d$ , then

$$\begin{aligned}
&F_\mu(\mathbf{w}_1) - F_\mu(\mathbf{w}_2) - \langle \nabla F_\mu(\mathbf{w}_2), \mathbf{w}_1 - \mathbf{w}_2 \rangle \\
&= \frac{1}{A_d} \int_{\mathbb{S}^d} [F(\mathbf{w}_1 + \mu\mathbf{z}) - F(\mathbf{w}_2 + \mu\mathbf{z}) - \langle \nabla F(\mathbf{w}_2 + \mu\mathbf{z}), \mathbf{w}_1 - \mathbf{w}_2 \rangle] d\mathbf{z} \\
&\geq \frac{1}{A_d} \int_{\mathbb{S}^d} \frac{\lambda}{2} \|\mathbf{w}_1 - \mathbf{w}_2\|_2^2 \\
&= \frac{\lambda}{2} \|\mathbf{w}_1 - \mathbf{w}_2\|_2^2,
\end{aligned}$$

where  $A_d$  is the surface area of the unit sphere.  $\square$

**Lemma B.12.** Let  $\mathbf{w} \in \mathbb{R}^d$ ,

$$\mathbb{E}_{\mathbf{z} \sim \mathbb{S}^d} [\|\bar{\mathbf{g}}(\mathbf{w}, \mathbf{z})\|_2^2] \leq 2d\|\nabla F(\mathbf{w})\|_2^2 + \frac{L_F^2 \mu^2 d^2}{2}.$$

*Proof.* Let  $A_d$  be the surface area of the unit sphere  $\mathbb{S}^d$ , then

$$\begin{aligned}
\mathbb{E}_{\mathbf{z} \sim \mathbb{S}^d} [\|\bar{\mathbf{g}}(\mathbf{w}, \mathbf{z})\|_2^2] &= \frac{1}{A_d} \int_{\mathbb{S}^d} \frac{d^2}{4\mu^2} (F(\mathbf{w} + \mu\mathbf{z}) - F(\mathbf{w} - \mu\mathbf{z}))^2 \|\mathbf{z}\|_2^2 d\mathbf{z} \\
&= \frac{d^2}{4A_d \mu^2} \int_{\mathbb{S}^d} (F(\mathbf{w} + \mu\mathbf{z}) - F(\mathbf{w} - \mu\mathbf{z}))^2 d\mathbf{z} \\
&\stackrel{(i)}{\leq} \frac{d^2}{2A_d \mu^2} \left[ \int_{\mathbb{S}^d} (F(\mathbf{w} + \mu\mathbf{z}) - F(\mathbf{w}))^2 d\mathbf{z} + \int_{\mathbb{S}^d} (F(\mathbf{w} - \mu\mathbf{z}) - F(\mathbf{w}))^2 d\mathbf{z} \right] \\
&\stackrel{(ii)}{\leq} \frac{d^2}{A_d \mu^2} \left[ \int_{\mathbb{S}^d} (F(\mathbf{w} + \mu\mathbf{z}) - F(\mathbf{w}) - \langle \nabla F(\mathbf{w}), \mu\mathbf{z} \rangle)^2 d\mathbf{z} \right. \\
&\quad \left. + \int_{\mathbb{S}^d} (F(\mathbf{w} - \mu\mathbf{z}) - F(\mathbf{w}) + \langle \nabla F(\mathbf{w}), \mu\mathbf{z} \rangle)^2 d\mathbf{z} + 2 \int_{\mathbb{S}^d} (\langle \nabla F(\mathbf{w}), \mu\mathbf{z} \rangle)^2 d\mathbf{z} \right] \\
&\stackrel{(iii)}{\leq} \frac{d^2}{A_d \mu^2} \left[ 2A_d \frac{L_F^2 \mu^4}{4} + 2A_d \frac{\mu^2}{d} \|\nabla F(\mathbf{w})\|_2^2 \right]
\end{aligned}$$

where (i) and (ii) use the fact that  $(x + y)^2 \leq 2x^2 + 2y^2$  and (iii) uses both the  $L_F$ -smoothness of  $F$  and Lemma B.2.  $\square$

**Lemma B.13.** Let  $\mathbf{x} \in \mathbb{R}^d$  and  $\mathbf{z}_1, \mathbf{z}_2$  be independently sampled from  $\mathbb{S}^d$ , then

$$\mathbb{E}_{\mathbf{z}_1, \mathbf{z}_2 \sim \mathbb{S}^d} [|\mathbf{z}_1^t \mathbf{z}_2| (\mathbf{x}^\top \mathbf{z}_1)^2] \leq \frac{\|\mathbf{x}\|_2^2}{\sqrt{d^3}}$$

*Proof.* Consider

$$\mathbb{E}_{\mathbf{z}_1, \mathbf{z}_2 \sim \mathbb{S}^d} [|\mathbf{z}_1^t \mathbf{z}_2| (\mathbf{x}^\top \mathbf{z}_1)^2] = \mathbb{E}_{\mathbf{z}_1 \sim \mathbb{S}^d} [\mathbb{E}_{\mathbf{z}_2 \sim \mathbb{S}^d} [|\mathbf{z}_1^\top \mathbf{z}_2|] (\mathbf{x}^\top \mathbf{z}_1)^2]$$

Consider now the rotation matrix  $R \in \mathbb{R}^{d \times d}$  that rotates  $\mathbf{z}_1$  to  $\mathbf{e}_1$ . Due to the symmetry of the unit sphere  $\mathbb{S}^d$ , the two random variables  $\mathbf{z}_2$  and  $R\mathbf{z}_2$  are identically distributed. Then, since  $\langle \mathbf{z}_1, \mathbf{z}_2 \rangle = \langle R\mathbf{z}_1, R\mathbf{z}_2 \rangle$ ,

$$\begin{aligned} \mathbb{E}_{\mathbf{z}_1, \mathbf{z}_2 \sim \mathbb{S}^d} [(|\mathbf{z}_1^t \mathbf{z}_2| (\mathbf{x}^\top \mathbf{z}_1)^2)^2] &= \mathbb{E}_{\mathbf{z}_2 \sim \mathbb{S}^d} [|\mathbf{e}_1^\top \mathbf{z}_2|] \mathbb{E}_{\mathbf{z}_1 \sim \mathbb{S}^d} [(\mathbf{x}^\top \mathbf{z}_1)^2]^2 \\ &= \|\mathbf{x}\|_2^2 \mathbb{E}_{\mathbf{z}_2 \sim \mathbb{S}^d} [|\mathbf{e}_1^\top \mathbf{z}_2|] \mathbb{E}_{\mathbf{z}_1 \sim \mathbb{S}^d} [(\mathbf{e}_1^\top \mathbf{z}_1)^2]^2 \end{aligned}$$

by also applying the same rotation argument to  $\mathbf{x}$ .

Now, since for any  $\mathbf{z}$  sampled from the unit sphere  $\mathbb{S}^d$ , we have

$$\begin{aligned} 1 &= \mathbb{E}_{\mathbf{z} \sim \mathbb{S}^d} [\|\mathbf{z}\|^2] \\ &= \mathbb{E}_{\mathbf{z} \sim \mathbb{S}^d} \left[ \sum_{i=1}^d (z^{(i)})^2 \right] \\ &= \sum_{i=1}^d \mathbb{E}_{\mathbf{z} \sim \mathbb{S}^d} [(z^{(i)})^2]. \end{aligned}$$

By the symmetry of the unit sphere,  $\mathbb{E}_{\mathbf{z} \sim \mathbb{S}^d} [(z^{(i)})^2] = \frac{1}{d}$  for all  $i \in [d]$ , where  $z^{(i)}$  denotes the  $i$ -th coordinate of  $\mathbf{z}$ . Lastly, since

$$\begin{aligned} \mathbb{E}_{\mathbf{z} \sim \mathbb{S}^d} [(\mathbf{e}_1^\top \mathbf{z})^2] &= \mathbb{E}_{\mathbf{z} \sim \mathbb{S}^d} [(z^{(1)})^2] \\ &= \frac{1}{d}, \end{aligned}$$

and, by applying Jensen's inequality on the square root function,

$$\begin{aligned} \mathbb{E}_{\mathbf{z} \sim \mathbb{S}^d} [|\mathbf{e}_1^\top \mathbf{z}|] &= \mathbb{E}_{\mathbf{z} \sim \mathbb{S}^d} \left[ \sqrt{(\mathbf{e}_1^\top \mathbf{z})^2} \right] \\ &\leq \frac{1}{\sqrt{d}}, \end{aligned}$$

we obtain the statement in the lemma. □

**Lemma B.14.** Let  $a, b, c, d, \delta \in \mathbb{R}$ ,  $\delta > 0$ , such that

$$|a - c| \leq \delta, \quad |b - d| \leq \delta,$$

then

$$|ab - cd| \leq \frac{c^2 + d^2}{2} + 2\delta^2.$$

*Proof.*

$$\begin{aligned} |ab - cd| &= |ab - cb + cb - cd| \leq |a - c||b| + |c||b - d| \\ &\leq \delta(|d| + \delta) + |c|\delta \\ &= |c|\delta + |d|\delta + \delta^2 \\ &\leq \frac{c^2 + d^2}{2} + 2\delta^2, \end{aligned}$$

where the last inequality uses the fact that  $xy \leq \frac{x^2 + y^2}{2}$ . □

**Lemma B.15.** Let  $z_1, z_2$  be independently sampled from  $\mathbb{S}^d$ . Then

$$\mathbb{E}_{z_1, z_2 \sim \mathbb{S}^d} [\langle \bar{\mathbf{g}}(\mathbf{w}, z_1), \bar{\mathbf{g}}(\mathbf{w}, z_2) \rangle] \leq (1 + \sqrt{d}) \|\nabla F(\mathbf{w})\|_2^2 + 2L_F^2 \mu^2 d^2.$$

*Proof.* Let  $A_d$  be the surface area of the unit sphere  $\mathbb{S}^d$  and define  $\mathbb{S}_+^d(z) = \{\mathbf{x} : \mathbf{x} \in \mathbb{S}^d, \mathbf{z}^\top \mathbf{x} > 0\}$  and similarly  $\mathbb{S}_-^d(z) = \{\mathbf{x} : \mathbf{x} \in \mathbb{S}^d, \mathbf{z}^\top \mathbf{x} < 0\}$ , then

$$\begin{aligned} & \mathbb{E}_{z_1, z_2 \sim \mathbb{S}^d} [\langle \bar{\mathbf{g}}(\mathbf{w}, z_1), \bar{\mathbf{g}}(\mathbf{w}, z_2) \rangle] \\ &= \frac{d^2}{A_d^2} \left[ \int_{\mathbb{S}^d} \int_{\mathbb{S}_+^d(z_1)} \frac{F(\mathbf{w} + \mu z_1) - F(\mathbf{w} - \mu z_1)}{2\mu} \frac{F(\mathbf{w} + \mu z_2) - F(\mathbf{w} - \mu z_2)}{2\mu} \mathbf{z}_1^\top \mathbf{z}_2 dz_2 dz_1 \right. \\ & \quad \left. + \int_{\mathbb{S}^d} \int_{\mathbb{S}_-^d(z_1)} \frac{F(\mathbf{w} + \mu z_1) - F(\mathbf{w} - \mu z_1)}{2\mu} \frac{F(\mathbf{w} + \mu z_2) - F(\mathbf{w} - \mu z_2)}{2\mu} \mathbf{z}_1^\top \mathbf{z}_2 dz_2 dz_1 \right] \\ &\stackrel{(i)}{\leq} \frac{d^2}{A_d^2} \left[ \int_{\mathbb{S}^d} \int_{\mathbb{S}_+^d(z_1)} \left( \nabla F(\mathbf{w})^\top \mathbf{z}_1 \nabla F(\mathbf{w})^\top \mathbf{z}_2 + \frac{(\nabla F(\mathbf{w})^\top \mathbf{z}_1)^2 + (\nabla F(\mathbf{w})^\top \mathbf{z}_2)^2}{2} + 2L_F^2 \mu^2 \right) \mathbf{z}_1^\top \mathbf{z}_2 dz_2 dz_1 \right. \\ & \quad \left. + \int_{\mathbb{S}^d} \int_{\mathbb{S}_-^d(z_1)} \left( \nabla F(\mathbf{w})^\top \mathbf{z}_1 \nabla F(\mathbf{w})^\top \mathbf{z}_2 - \frac{(\nabla F(\mathbf{w})^\top \mathbf{z}_1)^2 + (\nabla F(\mathbf{w})^\top \mathbf{z}_2)^2}{2} - 2L_F^2 \mu^2 \right) \mathbf{z}_1^\top \mathbf{z}_2 dz_2 dz_1 \right] \\ &= \mathbb{E}_{z_1, z_2 \sim \mathbb{S}^d} \left[ \nabla F(\mathbf{w})^\top \mathbf{z}_1 \mathbf{z}_1^\top \mathbf{z}_2 \mathbf{z}_2^\top \nabla F(\mathbf{w}) + \left( \frac{(\nabla F(\mathbf{w})^\top \mathbf{z}_1)^2 + (\nabla F(\mathbf{w})^\top \mathbf{z}_2)^2}{2} + 2L_F^2 \mu^2 \right) |\mathbf{z}_1^\top \mathbf{z}_2| \right] \\ &\stackrel{(ii)}{\leq} d^2 \nabla F(\mathbf{w})^\top \mathbb{E}_{z_1, z_2 \sim \mathbb{S}^d} [\mathbf{z}_1 \mathbf{z}_1^\top \mathbf{z}_2 \mathbf{z}_2^\top] \nabla F(\mathbf{w}) + \mathbb{E}_{z_1, z_2 \sim \mathbb{S}^d} [|\mathbf{z}_1^\top \mathbf{z}_2| (\nabla F(\mathbf{w})^\top \mathbf{z}_1)^2 + 2L_F^2 \mu^2] \\ &\stackrel{(iii)}{\leq} d^2 \left( \frac{1}{d^2} + \frac{1}{\sqrt{d^3}} \right) \|\nabla F(\mathbf{w})\|_2^2 + 2L_F^2 \mu^2 d^2 \end{aligned}$$

where (i) uses Lemma B.14 in conjunction with the  $L_f$  smoothness property of  $F$  that  $|\frac{F(\mathbf{w} + \mu \mathbf{z}) - F(\mathbf{w} - \mu \mathbf{z})}{2\mu} - \langle \nabla F(\mathbf{w}), \mathbf{z} \rangle| \leq L_F \mu$  for any  $\mathbf{z} \in \mathbb{S}^d$ , (ii) uses the fact that  $|\mathbf{z}_1^\top \mathbf{z}_2| \leq 1$ , and (iii) uses Lemmas B.3 and B.13.  $\square$

**Lemma B.16.** Let  $\mathbf{w} \in \mathbb{R}^d$  and  $z_r$  independently sampled from  $\mathbb{S}^d$ ,  $r \in [k]$ ,

$$\mathbb{E}_{z_r \sim \mathbb{S}^d} \left[ \left\| \frac{1}{k} \sum_{r=1}^k \bar{\mathbf{g}}(\mathbf{w}, z_r) \right\|_2^2 \right] = \frac{(k-1)(1 + \sqrt{d}) + 2d}{k} \|\nabla F(\mathbf{w})\|_2^2 + 2L_F^2 \mu^2 d^2.$$

*Proof.*

$$\begin{aligned} & \mathbb{E}_{z_r \sim \mathbb{S}^d} \left[ \left\| \frac{1}{k} \sum_{r=1}^k \bar{\mathbf{g}}(\mathbf{w}, z_r) \right\|_2^2 \right] = \mathbb{E}_{z_r \sim \mathbb{S}^d} \left[ \frac{1}{k^2} \sum_{r=1}^k \sum_{s=1}^k \bar{\mathbf{g}}(\mathbf{w}, z_r)^\top \bar{\mathbf{g}}(\mathbf{w}, z_s) \right] \\ &\stackrel{(i)}{\leq} \frac{1}{k^2} [k(2d \|\nabla F(\mathbf{w})\|_2^2 + 2L_F^2 \mu^2 d^2) + k(k-1)((1 + \sqrt{d}) \|\nabla F(\mathbf{w})\|_2^2 + 2L_F^2 \mu^2 d^2)] \\ &= \frac{(k-1)(1 + \sqrt{d}) + 2d}{k} \|\nabla F(\mathbf{w})\|_2^2 + 2L_F^2 \mu^2 d^2, \end{aligned}$$

where (i) uses Lemmas B.12 and B.15  $\square$

Now we can proceed with the proof of Theorem 5.13.

Let's consider the  $t$ -th step of Algorithm 1, then, by repeating the same idea in the proof of Theorem 5.10, we have

$$\mathbb{E}_{Z^t} [\|\mathbf{w}^{t+1} - \mathbf{w}_\mu^*\|_2] \leq \underbrace{\mathbb{E}_{Z^t} \left[ \left\| \mathbf{w}^t - \eta \frac{1}{k} \sum_{r=1}^k \bar{\mathbf{g}}(\mathbf{w}, z_r^t) - \mathbf{w}_\mu^* \right\|_2 \right]}_{T_1} + \eta \Delta$$



The fundamental difference lies in how we bound the term  $T_1$ . Let  $\tau = \frac{2d+(k-1)(1+\sqrt{d})}{k}$

$$\begin{aligned}
& \mathbb{E}_{Z^t} \left[ \left\| \mathbf{w}^t - \eta \frac{1}{k} \sum_{r=1}^k \bar{\mathbf{g}}(\mathbf{w}, \mathbf{z}_r^t) - \mathbf{w}_\mu^* \right\|_2^2 \right] \\
&= \mathbb{E}_{Z^t} \left[ \left\| \mathbf{w}^t - \mathbf{w}_\mu^* \right\|_2^2 - 2\eta \left\langle \mathbf{w}^t - \mathbf{w}_\mu^*, \frac{1}{k} \sum_{r=1}^k \bar{\mathbf{g}}(\mathbf{w}, \mathbf{z}_r^t) \right\rangle + \eta^2 \left\| \frac{1}{k} \sum_{r=1}^k \bar{\mathbf{g}}(\mathbf{w}, \mathbf{z}_r^t) \right\|_2^2 \right] \\
&\stackrel{(i)}{=} \left\| \mathbf{w}^t - \mathbf{w}_\mu^* \right\|_2^2 - 2\eta \langle \mathbf{w}^t - \mathbf{w}_\mu^*, \nabla F_\mu(\mathbf{w}^t) \rangle + \eta^2 \tau \|\nabla F(\mathbf{w}^t)\|_2^2 + 2\eta^2 L_F^2 \mu^2 d^2 \\
&\stackrel{(ii)}{\leq} \left( 1 - \frac{2\eta\lambda L_F}{L_F + \lambda} \right) \left\| \mathbf{w}^t - \mathbf{w}_\mu^* \right\|_2^2 - \left( \frac{2\eta}{L_F + \lambda} - 2\eta^2 \tau \right) \|\nabla F_\mu(\mathbf{w}^t)\|_2^2 + 2\eta^2 \left( 1 + \frac{\tau}{4} \right) L_F^2 \mu^2 d^2 \\
&\stackrel{(iii)}{=} \left( 1 - \frac{\lambda}{(L_F + \lambda)\tau} \right) \left\| \mathbf{w}^t - \mathbf{w}_\mu^* \right\|_2^2 - \left( \frac{1}{L_F(\lambda + L_F)\tau} - \frac{1}{2L_F^2\tau} \right) \|\nabla F_\mu(\mathbf{w}^t)\|_2^2 + \frac{1}{2L_F^2\tau^2} \left( 1 + \frac{\tau}{4} \right) L_F^2 \mu^2 d^2 \\
&\stackrel{(iv)}{\leq} \left( 1 - \frac{\lambda}{(L_F + \lambda)\tau} \right) \left\| \mathbf{w}^t - \mathbf{w}_\mu^* \right\|_2^2 + \frac{1}{2\tau^2} \left( 1 + \frac{\tau}{4} \right) \mu^2 d^2
\end{aligned}$$

where (i) comes from Lemmas B.8 and B.16, (ii) comes from Lemmas B.6, B.10 and Assumption 5.12, (iii) comes from choosing  $\eta = \frac{1}{2\tau L_F}$  and (iv) comes from the fact that  $\lambda \leq L_F$ .

Then by applying Jensen's inequality on the square root function and using the fact that  $\sqrt{x+y} \leq \sqrt{x} + \sqrt{y}$  and  $\sqrt{1-x} \leq 1 - \frac{x}{2}$ , we can bound  $T_1$  as

$$\mathbb{E}_{Z^t} \left[ \left\| \mathbf{w}^t - \eta \frac{1}{k} \sum_{r=1}^k \bar{\mathbf{g}}(\mathbf{w}, \mathbf{z}_r^t, 0) - \mathbf{w}_\mu^* \right\|_2 \right] \leq \left( 1 - \frac{\lambda}{2(L_F + \lambda)\tau} \right) \left\| \mathbf{w}^t - \mathbf{w}_\mu^* \right\|_2 + \frac{\mu d}{\sqrt{2}\tau} \sqrt{1 + \frac{\tau}{4}}.$$

Thus,

$$\mathbb{E}_{Z^t} [\|\mathbf{w}^{t+1} - \mathbf{w}_\mu^*\|_2] \leq \left( 1 - \frac{\lambda}{2(L_F + \lambda)\tau} \right) \left\| \mathbf{w}^t - \mathbf{w}_\mu^* \right\|_2 + \frac{1}{2L_F\tau} \Delta + \frac{\mu d}{\sqrt{2}\tau} \sqrt{1 + \frac{\tau}{4}}.$$

We conclude the proof by taking the expectation over  $Z^{t-1}$  and recursively applying the inequality.

□